UNIVERSITÄTSKLINIKUM HAMBURG-EPPENDORF

Klinik und Poliklinik für Neurologie

Prof. Dr. med. Christian Gerloff

Netzwerktopologische Aspekte der cerebralen Mikroangiopathie

Dissertation

zur Erlangung des Grades eines Doktors der Medizin
an der Medizinischen Fakultät der Universität Hamburg.

vorgelegt von:

Marvin Petersen
geb. in Hofgeismar

Hamburg 2020

Angenommen von der
Medizinischen Fakultät der Universität Hamburg am: 13.04.2021

Veröffentlicht mit Genehmigung der
Medizinischen Fakultät der Universität Hamburg.

Prüfungsausschuss, der/die Vorsitzende: Prof. Dr. Simone Kühn

Prüfungsausschuss, zweite/r Gutachter/in: Prof. Dr. Götz Thomalla

Inhaltsverzeichnis

1 Network Localisation of White Matter Damage in Cerebral Small Vessel Disease

SCIENTIFIC REPORTS
nature research

OPEN

Network Localisation of White Matter Damage in Cerebral Small Vessel Disease

Marvin Petersen[1]✉, Benedikt M. Frey[1], Eckhard Schlemm[1], Carola Mayer[1], Uta Hanning[2], Kristin Engelke[2], Jens Fiehler[2], Katrin Borof[3], Annika Jagodzinski[3,4], Christian Gerloff[1], Götz Thomalla[1] & Bastian Cheng[1]

Cerebral small vessel disease (CSVD) is a widespread condition associated to stroke, dementia and depression. To shed light on its opaque pathophysiology, we conducted a neuroimaging study aiming to assess the location of CSVD-induced damage in the human brain network. Structural connectomes of 930 subjects of the Hamburg City Health Study were reconstructed from diffusion weighted imaging. The connectome edges were partitioned into groups according to specific schemes: (1) connection to grey matter regions, (2) course and length of underlying streamlines. Peak-width of skeletonised mean diffusivity (PSMD) - a surrogate marker for CSVD - was related to each edge group's connectivity in a linear regression analysis allowing localisation of CSVD-induced effects. PSMD was associated with statistically significant decreases in connectivity of most investigated edge groups except those involved in connecting limbic, insular, temporal or cerebellar regions. Connectivity of interhemispheric and long intrahemispheric edges as well as edges connecting subcortical and frontal brain regions decreased most severely with increasing PSMD. In conclusion, MRI findings of CSVD are associated with widespread impairment of structural brain network connectivity, which supports the understanding of CSVD as a global brain disease. The pattern of regional preference might provide a link to clinical phenotypes of CSVD.

Cerebral small vessel disease (CSVD) is a condition comprising clinical, histopathological and imaging features thought to arise from damage to small perforating brain vessels[1]. Imaging markers considered to be manifestations of CSVD are recent small subcortical infarcts, lacunes, white matter hyperintensities of presumed vascular origin (WMH), enlarged perivascular spaces and cerebral microbleeds. The clinical sequelae of CSVD constitute the condition's major relevance in the ageing western societies. As per current research, CSVD is associated with ischaemic and haemorrhagic stroke, cognitive decline, dementia, late-life depression as well as gait and urinary complaints[2–5]. However, open questions remain concerning the underlying pathophysiology and causal relations between CSVD and its clinical sequelae[6].

Neuroimaging techniques are at the forefront of modern investigations of brain diseases. They offer insights into pathophysiological characteristics of various neurological disorders and thus also provide valuable information about the link between CSVD and its sequelae. On T2-weighted MRI data, WMH are a typical manifestation, however, brain tissue damage in CSVD is known to extend beyond lesions detectable by visual analysis. Diffusion weighted and diffusion tensor magnetic resonance imaging (DWI and DTI) in particular is capable of detecting CSVD-induced microstructural brain changes not visible on conventional T2-weighted data. Specifically, patients with CSVD were found to have altered microstructural properties in lesional and perilesional tissue detectable by DWI and DTI[7–9]. Based on these findings, a surrogate marker for the extent of CSVD termed "peak-width of skeletonised mean diffusivity" (PSMD) was proposed to capture microstructural white matter damage beyond traditional markers such as the volume of WMH. Therefore, PSMD features superior quantification capabilities while being robustly computable compared to other common CSVD surrogate markers[10].

[1]Department of Neurology, University Medical Center Hamburg-Eppendorf, Hamburg, Germany. [2]Department of Diagnostic and Interventional Neuroradiology, University Medical Center Hamburg-Eppendorf, Hamburg, Germany. [3]Epidemiological study center, University Medical Center Hamburg-Eppendorf, Hamburg, Germany. [4]Department of General and Interventional Cardiology, University Heart and Vascular Center, Hamburg, Germany. ✉e-mail: mar.petersen@uke.de

Connectomes are the subject of investigation in structural brain network analysis. They represent DWI-based reconstructions of human brain networks composed of nodes and internodal connections called edges[11]. In terms of anatomical correlates, nodes refer to cortical or subcortical grey matter areas, whereas edges represent the interconnecting white matter fibre tracts. Connectomes can be analysed by mathematical models to assess the integrity of brain networks *in vivo* and thus enable the appreciation of structural alterations in neurological disorders. In CSVD, application of graph theoretical measures to connectome data revealed decreased global efficiency of information transfer mediating cognitive symptoms[12]. While this finding describes pathological changes in large-scale brain network topology, connectome analysis also allows for localisation of altered structural integrity beyond the analysis of topological network parameters. In this study, we aimed to specify the impact of CSVD on the structural brain architecture using PSMD as a surrogate marker for CSVD. We chose to focus on two major aspects of white matter fibre tracts represented by edges in the structural connectome: first, edges were grouped according to interconnected grey matter areas to localise changes in distant yet connected brain regions. Second, edges were analysed according to their course and length (short or long intrahemispheric, interhemispheric) to specify the individual vulnerability of underlying white matter tracts. We hypothesised that structural disintegration relating to CSVD would affect a wide range of edges in the connectome. These changes would, however, show predominance for brain areas known to be involved in brain functions impaired in patients with CSVD.

Methods

Study population – the Hamburg City Health Study. The Hamburg City Health Study (HCHS) is a single center prospective, epidemiologic cohort study with emphasis on imaging to improve the identification of individuals at risk for major chronic diseases and to improve early diagnosis and survival. A detailed description of the overall study design has been published separately[13]. In brief, 45,000 citizens of the city of Hamburg, Germany, between 45 and 74 years are invited to an extensive baseline evaluation. A subgroup with present cardiovascular risk factors undergoes standardised MRI brain imaging. For this study, we analysed the first 1,000 brain MRI datasets from the HCHS baseline visit.

Standard protocol approvals, registration and participants consents. The local ethics committee of the Landesärztekammer Hamburg (State of Hamburg Chamber of Medical Practitioners, PV5131) approved the HCHS and written informed consent was obtained from all participants. Good Clinical Practice (GCP), Good Epidemiological Practice (GEP) and the Declaration of Helsinki were the ethical guidelines that governed conduct of the study.

MRI acquisition. Images were acquired using a 3-T Siemens Skyra MRI scanner (Siemens, Erlangen, Germany). Measurements were performed adapting a protocol as described previously[14]. In detail, for single-shell diffusion weighted imaging (DWI), 75 axial slices were obtained covering the whole brain with gradients ($b = 1000\ s/mm^2$) applied along 64 noncollinear directions with the following sequence parameters: repetition time (TR) = 8500 ms, echo time (TE) = 75 ms, slice thickness (ST) = 2 mm, in-plane resolution (IPR) = 2 × 2 mm, anterior-posterior phase-encoding direction. For 3D T1-weighted anatomical images, rapid acquisition gradient-echo sequence (MPRAGE) was used with the following sequence parameters: TR = 2500 ms, TE = 2.12 ms, 256 axial slices, ST = 0.94 mm, and IPR = 0.83 × 0.83 mm. 3D T2-weighted fluid attenuated inversion recovery (FLAIR) images were measured with the following sequence parameters: TR = 4700 ms, TE = 392 ms, 192 axial slices, ST = 0.9 mm, and IPR = 0.75 × 0.75 mm.

Data preprocessing, connectome reconstruction and measurement of connectivity. All data was pre-processed using MRtrix 3.0 (http://www.mrtrix.org), Advanced Normalization Tools (ANTs, https://github.com/ANTsX/ANTs), the FMRIB Software Library 5.0.10 (FSL, https://fsl.fmrib.ox.ac.uk) and FreeSurfer 6.0 (https://surfer.nmr.mgh.harvard.edu)[15]. Preprocessing steps for connectome reconstruction included bias correction, brain extraction, parcellation via FreeSurfer and tractography based on constrained spherical deconvolution (CSD) with subsequent application of spherical-deconvolution informed filtering of tractograms (SIFT2)[16,17]. The detailed pipeline can be found in the supplementary materials. Network nodes were defined by parcellation of the grey matter areas in T1-weighted images according to the Desikan-Killiany atlas[18]. Connectomes were not thresholded prior to edge connectivity quantification[19]. Two nodes were assumed to be connected by an edge if DWI signal-derived streamlines were running between them.

We investigated and localised the impact on white matter integrity in different components of the structural connectome. Therefore, network edges were grouped into categories representing two general anatomical aspects of brain architecture. Firstly, edges were grouped according to their connection to cortical brain regions using a predefined anatomical atlas that was condensed into major sections of the cerebral cortex, specifically frontal, temporal, parietal, occipital, limbic, insular, subcortical and cerebellar grey matter (Fig. 1b and Supplementary Table S1)[20]. Every edge was then assigned to these two regions based on which it connects. Thus, every edge was assigned twice: For example, an edge connecting the occipital and frontal region was allocated to both regions also meaning that an edge could count to the same group twice if it connected two regions from that group. Secondly, edges were grouped based on their length and course inside or between the two hemispheres (short or long intrahemispheric, interhemispheric) as illustrated in Fig. 1. Edges were determined as either running inter- or intrahemispherically, according to whether they were connecting brain regions on the same or different hemispheres, respectively. For definition of edge length, median streamline length of all edges was determined and their median was applied as a cut-off value for streamline length in each participant individually assigning edges into categories of short (if equal or below median) and long (if above median) edges. These definitions de facto resulted in three categories of network edges: long interhemispheric, long intrahemispheric and short intrahemispheric (see Fig. 1a)

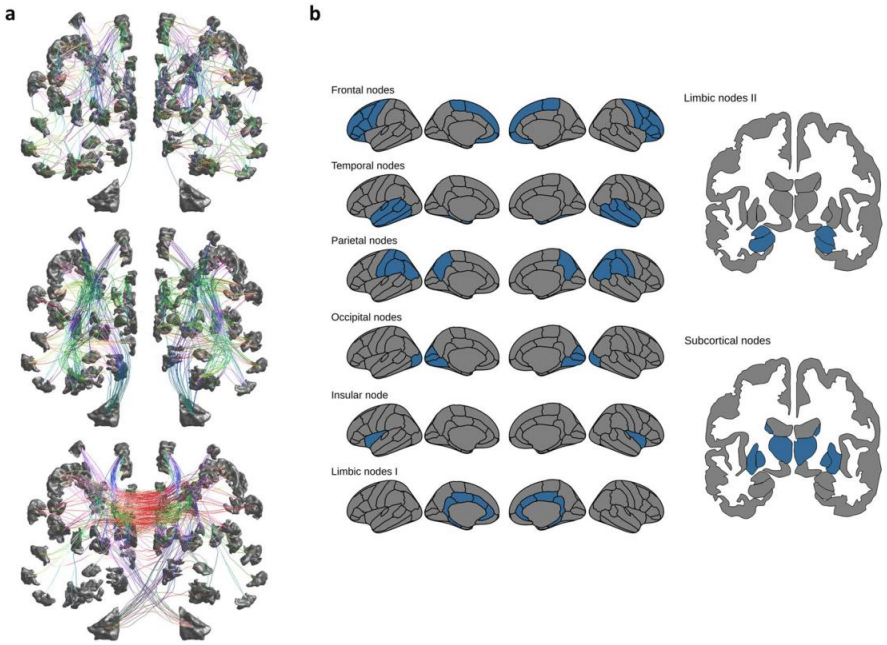

Figure 1. Illustration of edge grouping schemes applied in our study. Edges were grouped based on anatomical principles to investigate distinct impact of CSVD on different aspects of the human brain architecture. In **a**, the grouping by hemispheric course and length of edges is exemplarily illustrated from an anterior point of view. Grey areas represent nodes defined by atlas regions, edges are shown in colour coded by directional trajectory of white matter fibre tracts (X anterior-posterior, Y left-right, Z inferior superior). From top to bottom, intrahemispheric short edges, intrahemispheric long edges and interhemispheric edges are shown. In **b**, anatomical parcellations (grey areas) based on the Desikan atlas are shown. Edges were grouped by connectivity to a condensed selection of brain areas (blue). Abbreviations: CSVD = cerebral small vessel disease.

The individual edge connectivity was determined by summing up the weights of streamlines reaching from one node to the other with higher sums indicating increased connection strength, i. e., higher connectivity. Due to the application of SIFT2 the connectivity of an edge corresponds to the density of underlying fibres as estimated by CSD and is therefore interpreted by us as an indirect measure of white matter integrity[17]. Connectivity values were then summed up for each group of edges with respect to localisation (i. e., frontal or temporal edges) and course (i. e., long or short, intra- or interhemispheric edges). Again, higher values indicate increased connection strength in these separate groups of edges, whereas lower values point to decreases in connection strength. In addition, relative connectivity was computed by dividing an edge group's connectivity by the total connectivity of all edge groups.

Peak-width of skeletonised mean diffusivity computation. The PSMD tool provided at http://www.psmd-marker.com was used to compute PSMD[10]. The process consists of two steps. First, DTI data including mean diffusivity (MD) were skeletonised via Tract Based Spatial Statistics Procedure (TBSS)[21]. PSMD is the difference between the 95th and 5th percentiles of the MD voxel values within the skeleton.

White matter hyperintensity segmentation. We segmented WMH using the Brain Intensity AbNormality Classification Algorithm (BIANCA) implemented in FSL[22]. The training dataset consisted of masks of 100 participants and obtained by selecting only the voxels that were identified as WMH by two raters (MP, CM) independently via manual segmentation. White matter hyperintensity volumes were calculated.

Statistical analysis. Linear regression models were applied to assess associations between values of PSMD as a surrogate marker of CSVD and an edge group's connectivity. To account for the effects of age, sex and brain volume they were added as covariates to the linear models. Details regarding simple and multivariable linear models including actual p-values are listed in the supplementary materials (Supplementary Tables S2–S5). A formal interaction analysis served to ascertain the distinctiveness of the linear models ("connectivity ~ PSMD * fibre length group + (1|Subject)", "connectivity ~ PSMD * grey matter area + (1|Subject)", Supplementary Table S6). In addition, we calculated separate multivariable linear models including WMH load as defined as the volume of WMH normalised by individual brain volumes (Supplementary Tables S7 and S8). Statistical significance was defined as $p < 0.05$ and all p-values reported were corrected for multiple testing according to Bonferroni.

Female sex [n, (%)]	424 (45.6%)
Age [years], median (IQR)	64 (14)
Vascular risk factors	
Current smoking, [n, (%)]	167 (18.0%)
Hypertension (>= 140/90 mm/Hg), [n, (%)]	169 (18.2%)
Diabetes, [n, (%)]	74 (8.0%)
Conventional MRI measures	
Brain volume [ml], median (IQR)	1483.7 (203.1)
WMH volume [ml], median (IQR)	0.6 (1.4)
WMH load [%], median (IQR)	4.4 (9.8)
Diffusion imaging measures	
PSMD, median (IQR)	0.0002 (0.0001)
Connectome densitiy [%], median (IQR)	88 (3)

Table 1. Sample characteristics and image analysis results - the Hamburg City Health Study. Abbreviations: mm = millimeter, PSMD = peak-width of skeletonised mean diffusivity, WMH = white matter hyperintensities.

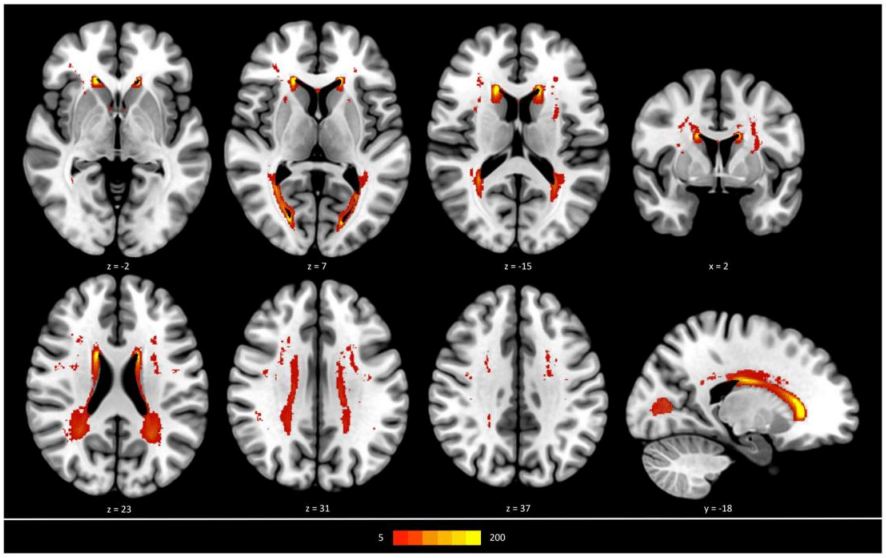

Figure 2. Distribution of white matter hyperintensities (in all participants, projected on a brain template in MNI-space. Frequency of WMH is illustrated as indicated by the colour bar. Z-values and Y-values refer to axial and sagittal slice position in MNI-space, respectively. Abbreviations: WMH = white matter hyperintensities.

Descriptive statistics of epidemiological and clinical data from all participants are provided as median and the interquartile range. The statistical analysis was performed in R (v3.1.4).

Results

Sample characteristics. In total, data from 1000 participants was available. After quality assessment of imaging data, 70 participants were excluded due to missing data (n = 21), poor quality or incompleteness (n = 40), or failed post-processing due to data incompatibility (n = 9). Thus, the analysis population encompassed 930 subjects. Epidemiological, clinical and imaging characteristics of all participants are shown in Table 1. Median age was 64 years (IQR = 14) and 45.6% of participants were female. Vascular risk factors were present in a considerable proportion of participants: arterial hypertension was present in 18.2% of participants, diabetes mellitus in 8.0% and 18.0% of participants were currently smoking.

Connectomes exhibited a median network density of 88% (IQR = 3%). Overall, the study sample showed only a minor to moderate lesion load with mainly periventricular distribution of WMH (see Fig. 2).

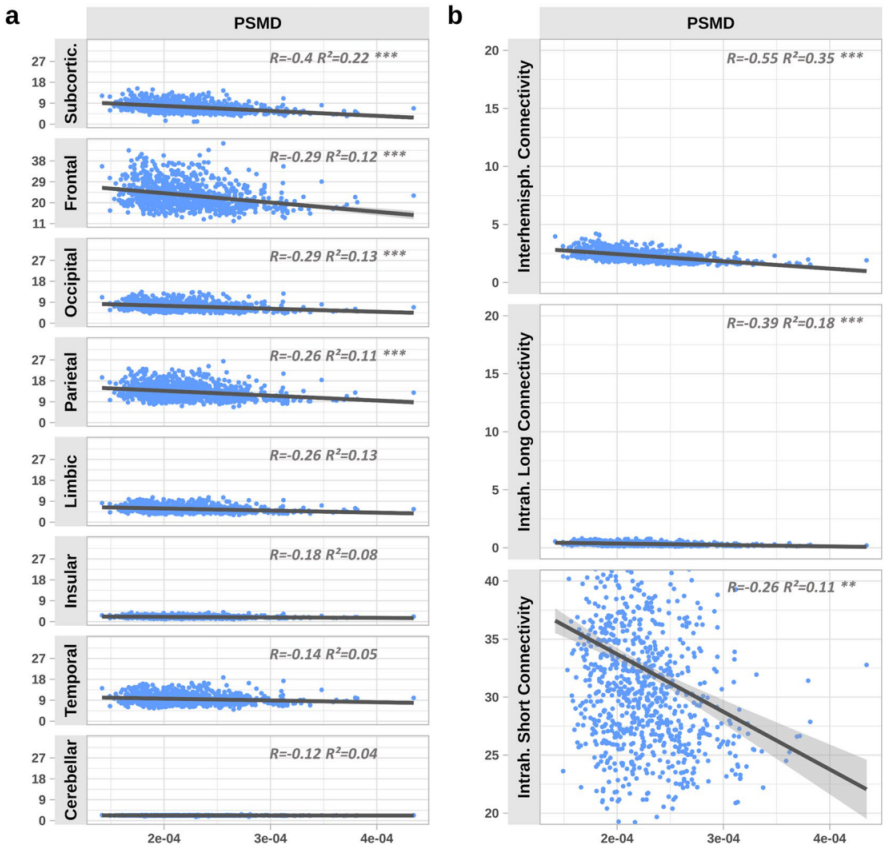

Figure 3. Effects of PSMD on edge groups connected by grey matter region (**a**) and hemispheric course and length (**b**). Simple linear regression results are shown using PSMD as independent and grey matter connectivities as well as course- and length-dependent connectivities as dependent variables. X-axis values correspond to the PSMD (no unit). Y-axis values correspond to the connectivity which represents the sum of all edge weights assigned to a respective group. R corresponds to the linear model before covariate inclusion whereas R^2 and significance levels (asterisks) correspond to the state after inclusion of covariates. Error bars show the 95% confidence interval. Figures are arranged from highest (top) to lowest (bottom) statistical association. (*$p < 0.1$; **$p < 0.05$; ***$p < 0.01$). Abbreviations: PSMD = peak-width of skeletonised mean diffusivity.

Connectivity analysis. *CSVD effects on grey matter area-specific connectivity.* Results from linear models are shown in Fig. 3a. Before covariate inclusion an increased PSMD was associated with a statistically significant decline of connectivity in all groups of edges. Here, the strongest effects were observed between PSMD and subcortical ($R = -0.4$, $p < 0.001$), frontal ($R = -0.29$, $p < 0.001$) and occipital connectivity ($R = -0.29$, $p < 0.001$). On the contrary, insular ($R = -0.18$, $p < 0.001$), temporal ($R = -0.14$, $p < 0.01$), and cerebellar connectivity ($R = -0.12$, $p < 0.05$) were of weakest correlation with PSMD (Supplementary Tables S2). After inclusion of age, sex and brain volume as covariates, correlations involving limbic, insular, temporal and cerebellar connectivity did not remain statistically significant (Supplementary Tables S3). Formal interaction analysis showed that all relationships regarding PSMD and investigated grey matter regions were of statistically significant difference (Supplementary Table S6). Computation of the relative connectivity indicated a preferential association of PSMD with decreased connectivity of subcortical and frontal brain regions: relative subcortical ($R = -0.48$, $p < 0.001$), frontal ($R = -0.14$, $p < 0.01$) connectivity exhibited negative correlations with PSMD, whereas the relative insular connectivity ($R = 0.23$, $p < 0.001$), temporal ($R = 0.45$, $p < 0.001$) and cerebellar ($R = 0.31$, $p < 0.001$) were positively correlated with PSMD (Supplementary Tables S4 *and* Fig. S1). After covariate inclusion these correlations remained significant (Supplementary Table S5).

CSVD effects on intra- or interhemispheric connectivity. The median cut-off to differentiate between long and short edges was 10.37 cm. Figure 3b illustrates the corresponding linear models. Interhemispheric ($R = -0.55$,

$p < 0.001$), long intrahemispheric ($R = -0.39$, $p < 0.001$) and short intrahemispheric ($R = -0.26$, $p < 0.001$) edge connectivity significantly decreased with higher PSMD levels (Supplementary Table S2*)*. Results remained significant after covariate inclusion (Supplementary Table S3). Formal interaction analysis showed that all relationships were of statistically significant difference (Supplementary Table S6). Moreover, PSMD correlated negatively with relative interhemispheric ($R = -.0.38$, $p < 0.001$) and intrahemispheric long edge connectivity ($R = -0.31$, $p < 0.001$), but positively with relative intrahemispheric short edge connectivity ($R = 0.43$, $p < 0.001$), thus indicating a specific association of higher PSMD with reduced interhemispheric and long intrahemispheric edge connectivity (Supplementary Table S4 and Fig. S1). These results remained significant after covariate inclusion aswell (Supplementary Table S5). Using WMH instead of PSMD as a predictor, multivariable linear models explained less variance of the observed connectivity data or showed non-significant correlations (Supplementary Tables S7 and S8).

Discussion

We report on the specific localisation of damage to the structural connectome associated with CSVD in a population-based sample of 930 subjects at increased risk for cerebrovascular diseases. We found that overall, CSVD was associated to a widespread decrease of structural connectivity. However, assessment of the relative connectivity indicated that the observed effects exhibited a regional preference. With regard to specific brain regions, edges connecting subcortical or frontal areas showed the most prominent decrease of connectivity in conjunction with higher CSVD burden as defined by PSMD. Regarding tract course and length, a preferential association of CSVD markers with decreased interhemispheric and long intrahemispheric connection integrity was found. These observations provide insights into structural brain network alterations associated with CSVD and advance the understanding of the pathophysiology of the disease itself and its clinical sequelae.

Effective communication between brain regions is accomplished by white matter pathways. Damage to these white matter pathways resulting from neurological or psychiatric disease hampers communication between brain areas and may further cause secondary damage by remote effects to cortical brain regions[23]. We observed significantly decreased connectivity along with increasing markers of CSVD in a considerable fraction of network edges indicating that a large proportion of white matter fibre pathways are indeed affected by CSVD. Of note, these changes were observed in our group of participants with relatively low WMH volumes compared to previous studies of patients with manifest cognitive impairment or extensive WMH[12,24]. Our findings point to widespread impairment of white matter integrity in the absence of extensive WMH detectable in T2-weighted MRI. Our results further demonstrate that despite of their apparent focal locality in the cerebral white matter, CSVD lesions are linked with disseminated structural changes in the brain architecture. This is in line with the recent perception of CSVD as a global instead of a focal brain disease[6].

In terms of anatomical localisation, our results showed that edges connecting subcortical or frontal brain regions are more prominently affected in subjects with higher CSVD burden. This was apparent in pronounced significant negative effects regarding subcortical and frontal relative connectivity, whereas in all other groups of edges, relative connectivities were of non-significant or positive association. We hypothesise that specific impairment of frontal and subcortical edges in CSVD are the structural determinants of prominent clinical sequelae such as impaired attention and executive brain functions. In line with our findings, previous studies reported frontal-subcortical pathophysiology in CSVD in terms of reduced glucose metabolism[25]. Lesion symptom inference analysis further indicated that WMH in regions of frontal-subcortical circuits can predict processing speed performance[26].

CSVD is considered to be among the main contributing factors to vascular cognitive impairment (VCI) and vascular dementia (VaD) which show specific clinical characteristics as compared to other types of dementia. VCI and VaD typically include executive dysfunction, impaired complex information handling and lowered self-control, which can be attributed to dysfunction in frontal brain networks, whereas compared to Alzheimer's disease the episodic memory deficits seem to be less severe[27–29]. However, how vascular pathology contributes to cognitive decline and dementia remains vague. One hypothesis is that cognitive decline originates from injury to fronto-subcortical pathways[30]. Moreover, it has been hypothesised that cognitive symptoms in CSVD are mediated by frontal atrophy[31,32]. Our findings are coherent with both theories. Frontal subcortical pathways could suffer by preferential frontal and subcortical fibre tract impairment in CSVD. Besides, damaged fibres could induce remote effects like frontal atrophy[14,33].

In terms of the course of white matter tracts, our observations indicate that interhemispheric and long-range connections are preferentially impaired by CSVD which is in line with findings of previous studies[12,24]. One probable explanation for this is the periventricular predominance of tissue damage in CSVD in close proximity to the course of long-range connections that run in an anterior-posterior trajectory. Accordingly, in our sample WMH, as a common CSVD manifestation, are primarily appearing in periventricular regions.

From a network perspective, interregional communication in the brain is reflected by the connectome's integrational capacity – i.e., the capability to integrate information from remote regions - which is demonstrably relevant for cognitive function[34,35]. The association between CSVD and cognitive dysfunction was found to be mediated by affection of integrational capacities[12]. Based on our results and the insight from both theoretical models on[36] and studies of stroke patients[37], that effective network integration is contingent on the integrity of long-range connections, we suggest that this mediation occurs through the disruptive effect of CSVD on white matter fibre tracts linking remote brain areas. Thus, our findings provide a further piece in the pathophysiological puzzle relating CSVD and cognitive decline.

Besides, functional network investigations indicate that decreased long-range connectivity is associated with Alzheimer's disease[38]. Conceivably, long-range connectivity is associated with cognitive symptoms across etiologies. Although recent work concludes that VaD and AD are affecting cognitive performance independently[39,40], our results support the hypothesis of pathophysiological overlap between both entities[41–43].

Strengths and limitations of our analysis. Strengths of this work lie in the large sample, and the state-of-the-art and reproducible neuroimaging pipeline. Applying PSMD values as a CSVD surrogate marker taking subvisible changes into account lead to increased explanatory precision in the linear regression analysis compared to the more commonly used measure of absolute WMH volumes.

The limitations are as follows. Although the sample has been risk-enriched by selection of subjects with a certain load of vascular risk factors, it stems from a population-based study and exhibits rather low burden of CSVD-associated lesions visible on structural MRI. Hence, investigations in a more severely affected sample might differ in results.

Since our analysis was focussed on investigating the location of CSVD-induced damage and thus deciphering the association of CSVD with patterns of connectome disruption without relating our findings to behaviour, we can only speculate on possible clinical implications of the observed associations.

Current methods of structural connectome reconstruction are an imperfect attempt to approximate white matter connections in the human brain. Although this methodology offers great advantages for *in-vivo* investigations of structural cerebral connectivity, this general limitation has to be considered when interpreting our results. Diffusion-to-axon mapping, i.e., inferring white matter fibre orientation and integrity from diffusion-weighted imaging, requires assumptions and approximations making it an indirect and error-prone process. A recent study compared state-of-the-art tractography methods by using synthetic data as a gold standard[44]. Accordingly, most approaches reconstruct a considerable amount of false positive streamlines including analysis pipelines very similar to ours. Using our approach, the probability that short streamlines are false positive is higher than for long streamlines. Even modern tractography approaches struggle to reconstruct complex fibre patterns like crossing, kissing, fanning and bending fibres because they lead to similar signal profiles within a voxel[45]. Besides tractography the observed results depend on further analysis design choices like the parcellation scheme underlying the nodes[46]. Our choice is informed by the wide usage of the Desikan-Killiany atlas to provide comparability and the rather coarse scheme increasing robustness of SIFT[47]. Not least, data quality has substantial impact on this type of analysis[46]. Since complex network analysis builds upon the reconstructed connectome, it inherits the shortcomings of the reconstruction approach because it builds upon it. Network characteristics such as global efficiency are abstract concepts that might oversimplify connectional patterns present in large-scale biological systems. However, alterations of large-scale network topology computed by graph theory have shown to be linked to clinical phenotypes of various neurological diseases and therefore present an innovative imaging biomarker in modern structural brain imaging studies[48]. Thus, we encourage the reader to interpret our results with the necessary care.

Future investigations. While this work limited on a topological approach to locate white matter alterations a fixel-based analysis allows to assess it in 3D space and thus displays a promising complementary approach. Moreover, future work might assess diffusion measurements in a sample not exhibiting any white matter hyperintensities, thus addressing the issue of white matter pathology beyond lesions accessible in T2-weighted MRI.

Conclusion

We demonstrated that in a sample of participants from a population-based study with an increased risk for vascular disease, white matter damage by CSVD is associated with widespread decreased structural brain connectivity. Specific parts of the structural connectome were preferentially affected. Decreases in connectivity were more pronounced in interhemispheric, long, frontal and subcortical edge groups. Our results link to the supposed pathophysiology of clinical sequelae of CSVD and shed further light on the underlying mechanisms of cognitive and depressive symptoms in CSVD in particular.

Data availability

Anonymised data of the analysis not published within this article will be made available on reasonable request from any qualified investigator after evaluation of the request by the Steering Board of the HCHS.

Received: 22 February 2020; Accepted: 11 May 2020;
Published online: 08 June 2020

References

1. Wardlaw, J. M. *et al.* Neuroimaging standards for research into small vessel disease and its contribution to ageing and neurodegeneration. *The Lancet Neurology* **12**, 822–838 (2013).
2. Pantoni, L. Cerebral small vessel disease: from pathogenesis and clinical characteristics to therapeutic challenges. *The Lancet Neurology* **9**, 689–701 (2010).
3. Debette, S. & Markus, H. S. The clinical importance of white matter hyperintensities on brain magnetic resonance imaging: systematic review and meta-analysis. *BMJ (Clinical research ed.)* **341**, c3666 (2010).
4. Rensma, S. P., van Sloten, T. T., Launer, L. J. & Stehouwer, C. D. A. Cerebral small vessel disease and risk of incident stroke, dementia and depression, and all-cause mortality: A systematic review and meta-analysis. *Neuroscience and Biobehavioral Reviews* **90**, 164–173 (2018).
5. Frey, B. M. *et al.* Characterization of White Matter Hyperintensities in Large-Scale MRI-Studies. *Front. Neurol.* **10** (2019).
6. ter Telgte, A. *et al.* Cerebral small vessel disease: from a focal to a global perspective. *Nature Reviews Neurology* **14**, 387–398 (2018).
7. Maillard, P. *et al.* White Matter Hyperintensity Penumbra. *Stroke* **42**, 1917–1922 (2011).
8. Maniega, S. M. *et al.* White matter hyperintensities and normal-appearing white matter integrity in the aging brain. *Neurobiology of Aging* **36**, 909–918 (2015).
9. van Norden, A. G. W. *et al.* Diffusion tensor imaging and cognition in cerebral small vessel disease: The RUN DMC study. *Biochimica et Biophysica Acta (BBA) - Molecular Basis of Disease* **1822**, 401–407 (2012).
10. Baykara, E. *et al.* A Novel Imaging Marker for Small Vessel Disease Based on Skeletonization of White Matter Tracts and Diffusion Histograms. *Annals of Neurology* **80**, 581–592 (2016).

11. Fornito, A. & Bullmore, E. T. Connectomics: A new paradigm for understanding brain disease. 733–748, https://doi.org/10.1016/j.euroneuro.2014.02.011 (2015).
12. Lawrence, A. J., Chung, A. W., Morris, R. G., Markus, H. S. & Barrick, T. R. Structural network efficiency is associated with cognitive impairment in small-vessel disease. *Neurology* **83**, 304 (2014).
13. Jagodzinski, A., Koch-gromus, U., Adam, G., Anders, S. & Augustin, M. Rationale and Design of the Hamburg City Health Study. *European Journal of Epidemiology*, https://doi.org/10.1007/s10654-019-00577-4 (2019).
14. Cheng, B. *et al.* Cortical atrophy and transcallosal diaschisis following isolated subcortical stroke. *Journal of Cerebral Blood Flow & Metabolism* 0271678X1983158, https://doi.org/10.1177/0271678X19831583 (2019).
15. Tournier, J.-D. *et al.* MRtrix3: A fast, flexible and open software framework for medical image processing and visualisation. *NeuroImage* **202**, 116137 (2019).
16. Jeurissen, B., Tournier, J.-D., Dhollander, T., Connelly, A. & Sijbers, J. Multi-tissue constrained spherical deconvolution for improved analysis of multi-shell diffusion MRI data. *NeuroImage* **103**, 411–426 (2014).
17. Smith, R. E., Tournier, J.-D., Calamante, F. & Connelly, A. SIFT2: Enabling dense quantitative assessment of brain white matter connectivity using streamlines tractography. *NeuroImage* **119**, 338–351 (2015).
18. Desikan, R. S. *et al.* An automated labeling system for subdividing the human cerebral cortex on MRI scans into gyral based regions of interest. (2006).
19. Civier, O., Smith, R. E., Yeh, C.-H., Connelly, A. & Calamante, F. Is removal of weak connections necessary for graph-theoretical analysis of dense weighted structural connectomes? *bioRxiv* 531350, https://doi.org/10.1101/531350 (2019).
20. Desikan, R. S. *et al.* An automated labeling system for subdividing the human cerebral cortex on MRI scans into gyral based regions of interest. (2006).
21. Smith, S. M. *et al.* Tract-based spatial statistics: Voxelwise analysis of multi-subject diffusion data. *NeuroImage* **31**, 1487–1505 (2006).
22. Griffanti, L. *et al.* BIANCA (Brain Intensity AbNormality Classification Algorithm): A new tool for automated segmentation of white matter hyperintensities. *NeuroImage* **141**, 191–205 (2016).
23. Lambert, C. *et al.* Longitudinal patterns of leukoaraiosis and brain atrophy in symptomatic small vessel disease. *Brain: a journal of neurology* **139**, 1136–51 (2016).
24. Tuladhar, A. M. *et al.* Disruption of rich club organisation in cerebral small vessel disease. *Human Brain Mapping* **38**, 1751–1766 (2017).
25. Tullberg, M. *et al.* White matter lesions impair frontal lobe function regardless of their location. *Neurology* **63**, 246–53 (2004).
26. Duering, M. *et al.* Strategic white matter tracts for processing speed deficits in age-related small vessel disease. *Neurology* **82**, 1946–50 (2014).
27. Wallin, A. *et al.* Update on Vascular Cognitive Impairment Associated with Subcortical Small-Vessel Disease. *Journal of Alzheimer's disease: JAD* **62**, 1417–1441 (2018).
28. Catani, M. *et al.* Beyond cortical localization in clinico-anatomical correlation. *CORTEX* **48**, 1262–1287 (2012).
29. Bennett, D. A., Gilley, D. W., Lee, S. & Cochran, E. J. White matter changes: neurobehavioral manifestations of Binswanger's disease and clinical correlates in Alzheimer's disease. *Dementia (Basel, Switzerland)* **5**, 148–52 (1994).
30. Román, G. C., Erkinjuntti, T., Wallin, A., Pantoni, L. & Chui, H. C. Subcortical ischaemic vascular dementia. *The Lancet Neurology* **1**, 426–436 (2002).
31. Mok, V. *et al.* Cortical and frontal atrophy are associated with cognitive impairment in age-related confluent white-matter lesion. *Journal of Neurology, Neurosurgery & Psychiatry* **82**, 52–57 (2011).
32. Schmidt, R. *et al.* White matter lesion progression, brain atrophy, and cognitive decline: The Austrian stroke prevention study. *Annals of Neurology* **58**, 610–616 (2005).
33. Tuladhar, A. M. *et al.* Relationship Between White Matter Hyperintensities, Cortical Thickness, and Cognition. *Stroke* **46**, 425–432 (2015).
34. Bassett, D. S. *et al.* Cognitive fitness of cost-efficient brain functional networks. *Proceedings of the National Academy of Sciences of the United States of America* **106**, 11747–52 (2009).
35. Heuvel, VanDen, Stam, M. P., Kahn, C. J. & Hulshoff Pol, R. S. H. E. Efficiency of functional brain networks and intellectual performance. *Journal of Neuroscience* **29**, 7619–7624 (2009).
36. Watts, D. J. & Strogatz, S. H. Collective dynamics of 'small-world" networks'. *Nature* **393**, 440–442 (1998).
37. Cheng, B. *et al.* Altered topology of large-scale structural brain networks in chronic stroke. *Brain Communications* **1** (2019).
38. Liu, Y. *et al.* Impaired long distance functional connectivity and weighted network architecture in Alzheimer's disease. *Cerebral cortex (New York, N.Y.: 1991)* **24**, 1422–35 (2014).
39. Koncz, R. & Sachdev, P. S. Are the brain's vascular and Alzheimer pathologies additive or interactive? *Current Opinion in Psychiatry* **31**, 147–152 (2018).
40. Roseborough, A., Ramirez, J., Black, S. E. & Edwards, J. D. Associations between amyloid β and white matter hyperintensities: A systematic review. *Alzheimer's & Dementia* **13**, 1154–1167 (2017).
41. Attems, J. & Jellinger, K. A. The overlap between vascular disease and Alzheimer's disease - lessons from pathology. *BMC Medicine* **12**, 206 (2014).
42. Love, S. & Miners, J. S. Cerebrovascular disease in ageing and Alzheimer's disease. *Acta Neuropathologica* **131**, 645–658 (2016).
43. Wallin, A. The Overlap between Alzheimer's Disease and Vascular Dementia: The Role of White Matter Changes. *Dementia and Geriatric Cognitive Disorders* **9**, 30–35 (1998).
44. Maier-Hein, K. H. *et al.* The challenge of mapping the human connectome based on diffusion tractography. *Nat Commun* **8**, 1–13 (2017).
45. Jbabdi, S. & Johansen-Berg, H. Tractography: Where Do We Go from Here? *Brain Connectivity* **1**, 169–183 (2011).
46. Sotiropoulos, S. N. & Zalesky, A. Building connectomes using diffusion MRI: why, how and but. *NMR in Biomedicine* **32**, e3752 (2019).
47. Smith, R. E., Tournier, J.-D., Calamante, F. & Connelly, A. The effects of SIFT on the reproducibility and biological accuracy of the structural connectome. *NeuroImage* **104**, 253–265 (2015).
48. Aerts, H., Fias, W., Caeyenberghs, K. & Marinazzo, D. Brain networks under attack: robustness properties and the impact of lesions. *Brain* **139**, 3063–3083 (2016).

Acknowledgements

The authors wish to acknowledge all participants of the Hamburg City Health Study and cooperation partners, patrons and the Deanery from the University Medical Center Hamburg - Eppendorf for supporting the Hamburg City Health Study. Special thanks applies to the staff at the Epidemiological Study Center for conducting the study. The participating institutes and departments from the University Medical Center Hamburg-Eppendorf contribute all with individual and scaled budgets to the overall funding. The Hamburg City Health Study is also supported by Amgen, Astra Zeneca, Bayer, BASF, Deutsche Gesetzliche Unfallversicherung (DGUV), DIFE, the Innovative medicine initiative (IMI) under grant number No. 116074 and the Fondation Leducq

under grant number 16 CVD 03., Novartis, Pfizer, Schiller, Siemens, Unilever and "Förderverein zur Förderung der HCHS e.V.". This work was supported by a grant from the German Research Foundation (Deutsche Forschungsgemeinschaft, DFG), Sonderforschungsbereich (SFB) 936, Project C2 (M.P., B.F., E.S., C.M., B.C. and G.T.). The publication has been approved by the Steering Board of the Hamburg City Health Study. Founding Board:Adam, Gerhard;Blankenberg, Stefan; Koch-Gromus, Uwe;Gerloff, Christian;Jagodzinski, Annika. List of Investigators:Adam, Gerhard;Aarabi, Ghazal;Augustin, Matthias; Behrendt, Christian; Beikler, Thomas; Betz, Christian;Blankenberg, Stefan; Bokemeyer, Carsten; Brassen, Stefanie; Brekenfeld, Caspar; Briken, Peer;Busch, Chia-Jung; Büchel, Christian; Debus, Eike Sebastian; Fiehler, Jens; Gallinat, Jürgen;Gellißen, Simone; Gerloff, Christian; Girdauskas, Evaldas; Gosau, Martin; Härter, Martin; Harth, Volker; Heydecke, Guido; Huber, Tobias; Jagodzinski, Annika; Johansen, Christoffer; Koch-Gromus, Uwe; Konnopka, Alexander; König, Hans-Helmut; Kromer, Robert; Kubisch, Christian; Kühn, Simone; Löwe, Bernd; Lund, Gunnar; Meyer, Christian; Nienhaus, Albert; Pantel, Klaus; Püschel, Klaus; Reichenspurner, Hermann; Sauter, Guido; Scherer, Martin; Schnabel, Renate; Schulz, Holger; Smeets, Ralf; Spitzer, Martin S.; Terschüren, Claudia;Thomalla, Götz; von dem Knesebeck, Olaf; Waschki, Benjamin; Wegscheider, Karl; Zeller, Tanja; Zyriax, Birgit-Christiane. Steering Board: Augustin, Matthias; Blankenberg, Stefan;Gallinat, Jürgen; Gerloff, Christian; Härter, Martin; Jagodzinski, Annika; Johansen, Christoffer; Koch-Gromus, Uwe; Sauter, Guido; Zeller, Tanja; Wegscheider, Karl; Betz, Christian; Heydecke, Guido; Gosau, Martin. Research consortium: Aarabi, Ghazal; Andrees, Valerie; Behrendt, Christian; Brassen, Stefanie; Brekenfeld, Caspar; Brünahl, Christian; Busch, Chia-Jung; Freitag, Janina; Gallinat, Jürgen; Gellißen, Susanne; Girdauskas, Evaldas; Heidemann, Christoph; Hussein, Yassin; Klein, Verena; Kofahl, Christopher; Kohlmann, Sebastian; Konnopka, Alexander; Kühn, Simone; Lühmann, Dagmar; Lund, Gunnar; Magnussen, Christina; Meyer, Christian;Nagel, Lina; Petersen, Elina; Scherschel, Katharina; Schiffner, Ulrich; Schnabel, Renate; Schulz, Holger; Seedorf, Udo; Smeets, Ralf; Terschüren, Claudia; Thomalla, Götz; Waschki, Benjamin; Zeller, Tanja; Zyriax, Birgit-Christiane.

Author contributions

The first author named is lead and corresponding author. We describe contributions to the paper using the CRediT contributor role taxonomy. Conceptualization: M.P., Data Curation: M.P., B.F., C.M.; Formal analysis: M.P., E.S.; Investigation: M.P., B.F., E.S., C.M., U.H., K.E., J.F., K.B., A.J., C.G., G.T., B.C.; Methodology: M.P., B.F., E.S.; Software: M.P., B.F., E.S.; Supervision: G.T., B.C.; Visualization: M.P.; Writing – original draft: M.P.; Writing – review & editing: M.P., B.F., E.S., C.M., U.H., K.E., J.F., K.B., A.J., C.G., G.T., B.C.

Competing interests

The authors declare no competing interests.

Additional information

Supplementary information is available for this paper at https://doi.org/10.1038/s41598-020-66013-w.

Correspondence and requests for materials should be addressed to M.P.

Reprints and permissions information is available at www.nature.com/reprints.

Publisher's note Springer Nature remains neutral with regard to jurisdictional claims in published maps and institutional affiliations.

2 White Matter Integrity and Structural Brain Network Topology in Cerebral Small Vessel Disease – the Hamburg City Health Study

White matter integrity and structural brain network topology in cerebral small vessel disease - the Hamburg City Health Study

Benedikt M. Frey[a*], Marvin Petersen[a*], Eckhard Schlemm[a], Carola Mayer[a], Uta Hanning[b], Kristin Engelke[b], Jens Fiehler[b], Katrin Borof[c], Annika Jagodzinski[c,d], Christian Gerloff[a], Götz Thomalla[a], Bastian Cheng[a]

[a] Department of Neurology, University Medical Center Hamburg-Eppendorf, Hamburg, Germany

[b] Department of Diagnostic and Interventional Neuroradiology, University Medical Center Hamburg-Eppendorf, Hamburg, Germany

[c] Epidemiological study center, University Medical Center Hamburg-Eppendorf, Hamburg, Germany

[d] Department of General and Interventional Cardiology, University Heart and Vascular Center, Hamburg, Germany

* Both authors contributed equally

Corresponding author:
Benedikt M. Frey
b.frey@uke.de
Department of Neurology
University Medical Center Hamburg-Eppendorf
Martinistraße 52, 22299 Hamburg, Germany

Abstract

Background

Cerebral small vessel disease is a common finding in the elderly and associated with a broad range of clinical sequelae. Previous studies suggest disturbances in the integration capabilities of structural brain networks as a mediating link between imaging and clinical presentations. To what extent cerebral small vessel disease might interfere with other measures of global network topology is not well understood.

Methods

Connectomes were reconstructed via diffusion weighted imaging in a sample of 930 participants from a population based epidemiologic study. Linear models were fitted testing for an association of graph-theoretical measures reflecting integration and segregation with both the Peak width of Skeletonized Mean Diffusivity (PSMD) and the load of white matter hyperintensities of presumed vascular origin (WMH). The latter were subdivided in periventricular and deep for an analysis of localisation-dependent correlations of cerebral small vessel disease.

Results

The median WMH volume was 0.6 ml (1.4) and the median PSMD 2.18 $mm^2/s \times 10^{-4}$ (0.5). The connectomes showed a median density of 0.880 (0.030), the median values for normalised global efficiency, normalised clustering coefficient, modularity Q and small-world propensity were 0.780 (0.045), 1.182 (0.034), 0.593 (0.026) and 0.876 (0.040) respectively. An increasing burden of cerebral small vessel disease was significantly associated with a decreased integration and increased segregation and thus decreased small-worldness of structural brain networks.

Conclusion

Even in rather healthy subjects increased cerebral small vessel disease burden is accompanied by topological brain network disturbances. Besides the known mediation effect of integration parameters, the segregation parameters might as well contribute to the understanding of the known clinical sequelae of cerebral small vessel disease.

Introduction

White matter hyperintensities of presumed vascular origin (WMH) are a common finding in MRI of elderly people and are a hallmark of cerebral small vessel disease (CSVD) [Wardlaw et al., 2013]. CSVD is considered to result from damage to small perforating arteries, arterioles, capillaries and venules of the human brain and represents an increasing burden in the ageing societies of industrialised countries [Pantoni, 2010; ter Telgte et al., 2018]. Besides rare hereditary causes, the major underlying pathology is arteriolosclerosis due to age and cardiovascular risk factors [Pantoni, 2010]. The clinical importance of CSVD lies in its association with various clinical sequelae such as ischaemic and haemorrhagic stroke, cognitive decline, dementia, late-life depression as well as gait and urinary complaints [Frey et al., 2019; Pantoni, 2010; Rensma et al., 2018; ter Telgte et al., 2018].

Findings from structural magnetic resonance imaging play a pivotal role in defining CSVD. The most common surrogate marker is the extent of WMH. However, this measure has some weaknesses such as the error-prone quantitative assessment of WMH via automated segmentation [Frey et al., 2019] as well as rather weak correlation with clinical symptoms [Baykara et al., 2016]. A novel surrogate marker of CSVD called ‘peak width of skeletonised mean diffusivity’ (PSMD) was suggested to overcome aforementioned limitations due to the robust nature of its computation and evidently strong correlations with clinical symptoms [Baykara et al., 2016; Wei et al., 2019]. The PSMD measures the distribution width of the mean diffusivity, i.e. the mean diffusion of water in all directions calculated by the diffusion tensor, in the white matter and thereby assesses the microstructural properties of the tissue. As WMH represent the part of the pathologic process visible on conventional MRI and thereby presumably only the tissue worst affected by CSVD, the PSMD particularly might be more sensitive to rather subtle pathologic changes in the microstructure of the brains white matter.

In recent years, growing evidence supports the understanding of the brain as a complex network of interconnected areas. The structural connectome as a comprehensive map of neuronal connections interprets the brain as a network based on two components: Nodes, which represent pre-specified cortical areas; and edges, representing the interconnecting white matter tracts [Fornito and Bullmore, 2015].

Connectomes allow inferences about the structural organisation and integrity of the human brain via graph theoretical analysis with global graph parameters reflecting topological network characteristics. As such, measures of segregation (e.g. the clustering coefficient and the modularity Q) reflect on the network's capability of distributed and parallel information processing, whereas measures of integration (e.g., global and local efficiency) give hints about the brain's capacities of combining information from such distributed processes.

The analysis of these global topological characteristics allows for the investigation of pathologic alterations in the structural network of the brain underlying neurological conditions like Alzheimer's, stroke and multiple sclerosis [Crofts et al., 2011; Stam, 2014; Stellmann et al., 2017]. In the context of CSVD, previous studies suggest disturbed topological network properties as a possible mechanism underlying clinical presentations in these patients [ter Telgte et al., 2018]. Decreased integration parameters were observed in particular and related to e.g. cognitive performance of the participants [Lawrence et al., 2014; Reijmer et al., 2015; Tuladhar et al., 2016b]. However, to what extent CSVD affects the degree of segregation in structural network topologies is less comprehensively studied.

The aim of this study was to investigate how brain network topology is affected by CSVD, namely the association of topological network parameters with the PSMD as a novel and robust marker of white matter integrity in CSVD and WMH load as the most common imaging markers representing CSVD. In addition, a deeper understanding of localisation-dependent correlations of CSVD was pursued by subdivision of WMH in periventricular (pWMH) and deep (dWMH).

Methods

Study design and participants

The Hamburg City Health Study (HCHS) is a single centre, prospective, epidemiologic cohort study with emphasis on imaging to improve the identification of individuals at risk for major chronic diseases and to improve early diagnosis and survival. A detailed description of the overall study design was published separately [Jagodzinski et al., 2019]. In summary, of all inhabitants living in Hamburg, a random sample is drawn from a total of 45,000 (aged 45-74) based on the official inhabitant data files. A written invitation to participate in HCHS is sent to their home address. All individuals willing to participate are invited to a baseline visit where they undergo an extensive assessment of their cardiovascular history and status. Of these, all participants with a Framingham stroke risk score (FSRS) of >7 points are invited to additional brain scans [Aparicio et al., 2017]. Furthermore, 1,500 healthy participants are selected for a control group. For an explorative analysis of cognitive functions, results from the „Mini Mental Status Test“ (MMST), the Trail Making Test part A (TMTA) and the Trail Making Test part B (TMTB) were selected. In addition, age, sex and years of educations were selected for analysis. For the present study, the MRI datasets of the first 1,000 participants undergoing imaging studies were selected - independent of FSRS. The local ethics committee approved the HCHS, and written informed consent was obtained from all participants.

MRI acquisition

Images were acquired using a 3-T Siemens Skyra MRI scanner (Siemens, Erlangen, Germany). For single-shell diffusion weighted imaging (DWI), 75 axial slices were obtained covering the whole brain with gradients (b = 1000 s/mm2) applied along 64 noncollinear directions with the following sequence parameters: repetition time (TR) = 8500 ms, echo time (TE) = 75 ms, slice thickness (ST) = 2 mm, in-plane resolution (IPR) = 2 × 2 mm, anterior-posterior phase-encoding direction. For 3D T1-weighted anatomical images, rapid acquisition gradient-echo sequence (MPRAGE) was used with the following sequence parameters: TR = 2500 ms, TE = 2.12 ms, 256 axial slices, ST = 0.94 mm, and IPR = 0.83 × 0.83 mm. 3D T2-weighted fluid attenuated inversion recovery (FLAIR) images were measured with the following sequence parameters: TR = 4700 ms, TE = 392 ms, 192 axial slices, ST = 0.9 mm, and IPR = 0.75 × 0.75 mm.

Quantification of CSVD

For segmentation of WMH, we used FSLs Brain Intensity AbNormality Classification Algorithm (BIANCA) [Griffanti et al., 2016], a fully automated, supervised k-nearest neighbour (k-NN) algorithm. The training dataset comprised masks of WMH for the first 100 participants. These masks were derived by selecting only the voxels that had been identified as WMH by two trained raters (MP and CM) independently with manual segmentation. The mean Dice Similarity Index between the segmentation of both raters was 0.63.

Derived masks of WMH were divided into periventricular (pWMH) and deep (dWMH) by a 10mm distance threshold to the ventricles [DeCarli et al., 2005; Griffanti et al., 2018]. WMH load was calculated as the share of WMH in the brain tissue volume (intracranial volume - ventricle volume) and logarithmised for further statistical analysis due to a right-skewed distribution. Logarithmic pWMH respectively dWMH load were calculated analogously.

PSMD was calculated with the available original scripts on diffusion tensor imaging (DTI) data (http://www.psmd-marker.com, [Baykara et al., 2016]). In brief, the pre-calculated maps of MD were brought to MNI space using the coregistration of the pre-calculated FA maps with the FSL-TBSS package [Smith et al., 2006]. Following white matter tract skeletonisation of the standardised MD maps, the PSMD was calculated via histogram analysis.

Connectome reconstruction

All imaging data was processed using MRtrix 3.0 ([Tournier et al., 2019], http://www.mrtrix.org), Advanced Normalization Tools (ANTs, https://github.com/ANTsX/ANTs), the FMRIB Software Library 5.0.10 (FSL, https://fsl.fmrib.ox.ac.uk) and FreeSurfer 6.0 (https://surfer.nmr.mgh.harvard.edu). Network nodes were defined by parcellation of the grey matter areas in T1w according to the Desikan-Killiany and Aseg atlas [Desikan et al., 2006; Filipek et al., 1994] including a total of 84 cortical and subcortical regions. There was no anatomical overlap between brain regions considered as nodes in the analysis. DWI preprocessing involved denoising, removal of Gibbs ringing artifacts, eddy current correction and motion correction, bias field correction as well as susceptibility distortion correction based on nonlinear registration [Andersson and Sotiropoulos,

2016; Avants et al., 2008; Kellner et al., 2016; Tustison et al., 2010; Veraart et al., 2016]. Constrained spherical deconvolution and anatomically constrained tractography (ACT) [Smith et al., 2012] allowed for streamlines reconstruction from preprocessed diffusion images. Upon that streamlines were filtered by spherical deconvolution informed filtering of tractograms (SIFT2) [Smith et al., 2015]. Two nodes were assumed to be connected by an edge if DWI signal-derived streamlines were running between them. The edge weight was determined by the weighted streamline count reaching from one node to the other. The detailed pipeline and an illustration of regions of interests derived from the atlases and used for node definition can be found in the supplementary materials.

Connectome analysis

Connectomes produced were further processed with the brain connectivity (BCT) toolbox [Rubinov and Sporns, 2010] in matlab (v2018b). This included connectome normalisation and global graph parameter computation. The following topological global graph parameters have been extracted: global efficiency, clustering coefficient, modularity Q and small-world propensity. The graph parameters are explained in Box 1. The global efficiency and clustering coefficient are sensitive to low level features of the connectomes as they are derived from the value of connection weights and degree distribution. To account for this dependency, both were normalised against graph parameters derived from and averaged over 100 null models which were acquired by randomly rewiring subject connectomes preserving the degree distribution [Maslov et al., 2002]. Corresponding standard errors are listed in the results. Furthermore, the network density, i.e. the fraction of present and possible connections, and median edge weight, i.e. the median of all connection weights, were computed for all participants.

Statistical analysis

The statistical analysis has been performed in R (v3.1.4). To assess the associations of the CSVD surrogate markers with global graph parameters, a linear regression analysis was performed. For facilitated interpretability effects of simple linear regressions are conveyed in the first place. Subsequently, we report whether significance remains after correcting for age, sex, brain volume and median edge weight. To compare the correlations of pWMH and dWMH regarding the global graph

parameters, Pearson and Filon's z was applied [Diedenhofen and Musch, 2015]. For an explorative analysis of associations with cognitive functions, simple and multivariable linear regression models adjusted for age, sex and years of education were fitted for the association between performance in MMST, TMT-A and TMT-B with global graph parameters and CSVD surrogate markers, respectively. Unless stated otherwise, descriptive statistics are given as median with interquartile range (IQR).

Data assessment and quality assurance

The quality of the initial data and the reliability of the relevant processing steps in our pipeline were assessed repeatedly. DWI-data was initially checked for completeness of the sequence and signal-to-noise ratio, mean voxel intensity, outlier count and maximum voxel intensity outlier count were calculated [Roalf et al., 2016]. Finally, the output statistics of the outlier replacement step of FSL's eddy were used for additionally identifying data with poor quality.

Results

Sample characteristics

Descriptive statistics are listed in *table 1*. Due to missing data and after quality assessment, the final sample for this study comprised 930 participants. 21 participants were excluded due to missing imaging data, 40 participants were excluded due to poor quality or incompleteness of imaging data (39 DWI, 1 FLAIR) and 9 participants were excluded due to poor quality of certain processing steps. The median subject age was 64 years (IQR = 14), 45.6% were women. *Figure 1* depicts a heatmap delineating the spatial distribution of WMH, the median WMH volume was 0.6 ml (1.4) and the median PSMD 2.18 mm2/s x 10^{-4} (0.5). The structural connectomes showed a median density of 0.880 (0.030), the median values for normalised global efficiency, normalised clustering coefficient, modularity Q and small-world propensity were 0.780 (0.045), 1.182 (0.034), 0.593 (0.026) and 0.876 (0.040) respectively. The median score for the MMST was 28 points (2), the median time for the TMTA was 36 seconds (17) and 79 seconds (37) for the TMTB. A mean connectome matrix can be found in the supplementary materials.

Association of CSVD surrogate markers with global graph parameters

Simple linear regression analysis of the relationship between CSVD surrogate markers and global graph parameters revealed consistent and statistically significant correlations which are illustrated in *figure 2*. The normalised global efficiency (R=-0.66, p<0.001) and small-world propensity (R=-0.57, p<0.001) were negatively correlated with PSMD. Normalised clustering coefficient (R=0.46, p<0.001) and modularity Q (R=0.37, p<0.001) were positively correlated with PSMD. Correlations of log WMH load, log pWMH load and log dWMH load with global graph parameters exhibited smaller effect sizes and significance levels. After correcting for age, sex, brain tissue volume, median edge weight and cardiovascular risk factors, all but the following correlations remained significant: WMH load with respect to the modularity (p=0.115), dWMH load with respect to global efficiency (p=0.422) and small-world propensity (p=0.614) as well as pWMH load with respect to clustering coefficient (p=0.104) and modularity (p=0.155) remained significant. Applying Pearson and Filon's Z for correlation comparison revealed that global efficiency (R=-0.39 vs R=-0.19, p<0.001) as well as small world propensity (R=-0.32 vs R=-0.16, p<0.001) correlated significantly stronger with pWMH load than with dWMH load. Correlations of pWMH and dWMH with the normalised clustering coefficient (p=0.177) and modularity Q (p=0.398) showed no statistically significant difference. Further details of the linear regression results are listed in the supplementary materials.

Analysis of cognitive function, CSVD surrogate markers and global graph parameters

MMST was found to be associated with PSMD (simple regression analysis p=0.017 and multivariable analysis p=0.244, respectively), pWMH (p=0.020 and p=0.789, respectively), global efficiency (p=0.019 and p=0.599, respectively) and modularity Q (p=0.013 and p=0.281, respectively). There was no association of MMST and dWMH (p=0.191 and p=0.956, respectively), Clustering coefficient (p=0.263 and p=0.957, respectively) and small-world propensity (p=0.053 and p=0.637, respectively).

TMTA was found to be associated with PSMD (p<0.001 and p=0.021, respectively), pWMH (p<0.001 and p=0.059, respectively), dWMH (p<0.001 and p=0.005, respectively), global efficiency (p<0.001 and p=0.009, respectively), modularity Q (p<0.001 and p=0.059, respectively) and small-world propensity (p<0.001 and p=0.002, respectively). There was no association of TMTA and Clustering coefficient

(p=0.083 and p=0.877, respectively). After correcting for multiple testing, only the association with small-world propensity remained significant.

TMTB was found to be associated with PSMD (p<0.001 and p<0.001, respectively), pWMH (p<0.001 and p=0.315, respectively), dWMH (p<0.001 and p=0.185, respectively), global efficiency (p<0.001 and p=0.006, respectively), Clustering coefficient (p<0.001 and p=0.058, respectively), modularity Q (p<0.001 and p=0.014, respectively) and small-world propensity (p<0.001 and p<0.001, respectively). After correcting for multiple testing, only the association with small-world propensity and PSMD remained significant.

Discussion

In this analysis of a population-based sample of 930 subjects, we investigated the association of CSVD with brain network topology using state of the art methodology to reconstruct structural connectomes derived from DWI and structural imaging data. As a main finding, we identified a significant association of CSVD burden with decreased integration and increased segregation of structural brain networks resulting in a weakened small-world structure. These findings provide novel insights into the effects of CSVD on the architecture and integrity of brain networks and may foster the understanding of the clinical sequelae of CSVD.

Association of CSVD with global graph parameters

Recent research provided evidence about the topological properties of the underlying network organisation of the human brain [Latora and Marchiori, 2001; Sporns and Zwi, 2004]. Accordingly, the human brain is organised in a topological paradigm called ‘small world’ as it applies to most real-world networks [Costa et al., 2011]. Small-worldness describes a compromise between pronounced segregation, meaning that distributed and specialised processing happens in subsections of the brain, and integration, the brain’s capacity of integrating information from distributed processes [Watts and Strogatz, 1998]. Hence a networks small-worldness is immediately depending on sufficient integration and segregation characteristics. To investigate the network topology of the reconstructed connectomes and its alteration by CSVD, topological network parameters were assessed and related to PSMD as a novel and robust surrogate parameter of white matter integrity and WMH load as the most common imaging marker representing CSVD. The investigated connectomes were of

strong small-worldness as the mean small-world propensity of 0.87 was above the suggested threshold of 0.6 [Muldoon et al., 2016]. It turned out that the integration parameter - global efficiency - decreases while the segregation parameters - clustering coefficient and modularity Q - increase with higher CSVD burden. Both phenomena ultimately result in weakening of small-world topology as a relatively low small-world propensity accompanies high CSVD burden. To put this into context, the observed alterations of brain network topology might suggest that the brain's capacity of integrating distributed information decreases, while the capability of distributed computation increases with higher CSVD burden. We found that periventricular WMH (pWMH) drive the reduction of integration capabilities and small-worldness overall, showing significantly higher effects than deep white matter WMH (dWMH). The effects of dWMH on segregation parameters were of statistical significance whereas the effects of pWMH were not. Since long-range connections are preferentially passing through ventricle-near regions [Brodal, 2016], the observed topological alterations might be explained by a disproportionate decrease of long-range connections in CSVD as suggested in previous studies in this cohort of participants of the HCHS [Petersen et al., 2020].

Global efficiency depends on the integrity of these long-distance connections, as these connections enable communication of remote brain regions [Watts and Strogatz, 1998]. Hence a reduction of these fibres might explain the reduced global efficiency we observed in subjects with high CSVD burden. This is in line with the hypothesis that primarily pWMH are responsible for global efficiency decline and therefore the cognitive decline in CSVD patients, as supported by other studies [Cees De Groot et al., 2000].

The increased clustering coefficient and modularity might be attributable to affected long-range connections as well. Provided they are underrepresented, long-range connections might lead with higher probability to open triangles, respectively less modular structure, decreasing the average clustering coefficient and modularity. Conversely, less long-range connections might yield higher segregation parameters. Moreover, in presence of CSVD pathology the normal appearing white matter (NAWM) fibre density might increase compensatorily yielding more intensively connected node neighborhoods and modules, as hypothesised in stroke patients [Crofts et al., 2011; Dancause et al., 2005].

Importance of global graph parameters for clinical sequelae of CSVD

These findings are of clinical relevance hence they might illuminate how associations between CSVD and its known clinical sequelae are mediated. A lower global efficiency, regardless of health status, is associated with poorer cognitive performance [Bassett et al., 2009; Berlot et al., 2016; Heuvel et al., 2009; Li et al., 2009]. In line with this, recent studies found that the interrelation of CSVD occurrence and cognitive decline is mediated by a decreased global efficiency [Lawrence et al., 2014; Tuladhar et al., 2016a; Tuladhar et al., 2016b]. In our study, we found only a rather weak association of global graph parameters with the cognitive performance after correction for multiple testing - we assume mostly due to the modest variance in our rather healthy cohort.

Looking beyond cognition, results from other cohort studies back the assumption that late-life depression is associated with CSVD, summarised as the vascular depression hypothesis [Alexopoulos, 2006]. Depressive CSVD patients were found to have a significantly decreased global efficiency compared to patients without depressive symptoms [Xie et al., 2017]. However, no mediation effect of the brain's integration capabilities could be verified in this study, due to the small percentage of participants demonstrating signs of depression (N=20).

PSMD versus WMH as surrogate markers for CSVD

Previous studies using diffusion weighted imaging (DWI) report that CSVD patients exhibit a higher mean diffusivity (MD), meaning an increased diffusion magnitude, as well as a decreased fractional anisotropy (FA), suggesting a decreased directionality of diffusion [van Norden et al., 2012; Tuladhar et al., 2016a]. These findings might reflect a decreased fibre integrity and pathologic aggregation of free water in the extracellular compartment [Duering et al., 2018] and indicate that DWI is able to reflect microstructural changes caused by CSVD. Based on comparison of the linear models R^2 values, our analysis suggests a superior explanatory power of PSMD compared to the different WMH loads with regard to the global efficiency, clustering coefficient and small-world propensity. This observation may be owed to the robust calculation of the PSMD in contrast to the error-prone nature of WMH segmentation. The algorithm we used for the automated segmentation of WMH tends to underestimate dWMH [Griffanti et al., 2016], potentially blurring the influence of WMH load on the topological network properties. As mentioned before, the PSMD might be more sensitive to rather subtle

microstructural pathologies. The moderate CSVD burden in our study sample might therefore favour the PSMD, as the median WMH volumes were rather low compared to other cohort studies investigating CSVD. These results accentuate the PSMD's high capability of capturing CSVD severity - even in brains appearing healthy on conventional MRI [Baykara et al., 2016].

Methodological considerations on structural connectome reconstruction

Weighted structural connectomes were successfully reconstructed in all participants. Our connectomes exhibited a rather high density with regard to comparable previous studies [Lawrence et al., 2014; Tuladhar et al., 2016a; Tuladhar et al., 2016b] which is owed to our usage of the '2nd order integration over fibre orientation distributions 2'-algorithm (iFOD2) [Tournier, J.-D. Calamante, F. & Connelly, 2010] during tractography without a separate thresholding step [Civier et al., 2019]. Tract-tracing studies of macaque brains yielded similarly densely connected connectomes suggesting biological plausibility and accuracy of the type of connectome used in this study [Markov et al., 2011].

Strength and limitations of our study

Briefly, advantageous features of this work lie in the utilisation of PSMD as a CSVD surrogate parameter, the size of the sample and a state of the art and reproducible processing pipeline applied to it.

Our study has limitations. Even though the cohort represents a population with increased cardiovascular risk, the overall analysed participants were relatively healthy regarding imaging findings of CSVD. Findings might be different in a more severely affected sample. However, we would argue that our findings in a group of patients with relatively mild degree of CSVD point towards changes in white matter microstructure and disturbances of brain network topology already detectable at an early stage of CSVD. As we think of CSVD as a chronic-progressive disease, it is likely that other graph parameters calculated in this study would follow characteristic trajectories depending on disease progression. Extrapolation to datasets with patients in more advanced stages of CSVD would most certainly be possible for the Clustering Coefficient, which is strongly dependent on overall connectivity strength (reflecting progressing loss of structural white matter integrity in CSVD). However, Modularity and Small World Propensity are parameters in graph theory more sensitive to

topological network changes (specific anatomical pattern of white matter degeneration). Therefore, hypotheses regarding the translation of findings in our group to more severely affected patients cannot be tested validly in the current sample

Conclusion

To summarise, in a large sample of subjects with vascular risk factors we were able to demonstrate that CSVD is associated with alteration of structural brain network topology considered crucial for maintenance of proper brain function – independently from the used surrogate parameter. Higher burden of CSVD goes along with a shift of brain network topology towards reduced integration, which might reflect the pathology underlying impaired cognitive function in CSVD and an increased segregation and consequently altered small-world structure. These findings might reflect a pathology of the brain network functionality in CSVD that could explain the associated sequelae. Since the clinical impacts of increased segregation are not well understood yet, these parameters might serve as a promising subject for future studies in CSVD patients.

Acknowledgements and conflicts of interest

We describe contributions to the paper using the CRediT contributor role taxonomy. Conceptualization: BF, MP; Data Curation: BF, MP, CM; Formal analysis: BF, MP, ES; Investigation: all; Methodology: BF, MP, ES; Software: BF, MP, ES; Supervision: GT, BC; Visualization: BF, MP; Writing – original draft: BF, MP; Writing – review & editing: BF, MP, ES, CM, GT, BC.

The publication has been approved by the Steering Board of the Hamburg City Health Study.

The authors wish to acknowledge all participants of the Hamburg City Health Study and cooperation partners, patrons and the Deanery from the University Medical Centre Hamburg - Eppendorf for supporting the Hamburg City Health Study. Special thanks applies to the staff at the Epidemiological Study Center for conducting the study. The participating institutes and departments from the University Medical Center Hamburg-Eppendorf contribute all with individual and scaled budgets to the overall funding. The Hamburg City Health Study is also supported by Amgen, Astra Zeneca, Bayer, BASF, Deutsche Gesetzliche Unfallversicherung (DGUV), DIFE, the Innovative medicine initiative (IMI) under grant number No. 116074 and the Fondation Leducq under grant

number 16 CVD 03., Novartis, Pfizer, Schiller, Siemens, Unilever and “Förderverein zur Förderung der HCHS e.V.”.

Dr. Thomalla reports receiving consulting fees from Acandis, grant support and lecture fees from Bayer, lecture fees from Boehringer Ingelheim, Bristol-Myers Squibb/Pfizer, and Daiichi Sankyo, and consulting fees and lecture fees from Stryker; Dr. Gerloff, receiving lecture fees and advisory board fees from Boehringer Ingelheim. Dr. Fiehler, receiving consulting fees from Acandis, Cerenovus, Medtronic, Microvention, Penumbra, and Route 92 Medical.

Founding Board:
Adam, Gerhard
Blankenberg, Stefan
Koch-Gromus, Uwe
Gerloff, Christian
Jagodzinski, Annika

List of Investigators:
Adam, Gerhard
Aarabi, Ghazal
Augustin, Matthias
Behrendt, Christian
Beikler, Thomas
Betz, Christian
Blankenberg, Stefan
Bokemeyer, Carsten
Brassen, Stefanie
Brekenfeld, Caspar
Briken, Peer
Busch, Chia-Jung
Büchel, Christian
Debus, Eike Sebastian
Fiehler, Jens
Gallinat, Jürgen

Gellißen, Simone
Gerloff, Christian
Girdauskas, Evaldas
Gosau, Martin
Härter, Martin
Harth, Volker
Heydecke, Guido
Huber, Tobias
Jagodzinski, Annika
Johansen, Christoffer
Koch-Gromus, Uwe
Konnopka, Alexander
König, Hans-Helmut
Kromer, Robert
Kubisch, Christian
Kühn, Simone
Löwe, Bernd
Lund, Gunnar
Meyer, Christian
Nienhaus, Albert
Pantel, Klaus
Püschel, Klaus
Reichenspurner, Hermann,
Sauter, Guido
Scherer, Martin
Schnabel, Renate
Schulz, Holger
Smeets, Ralf
Spitzer, Martin S.
Terschüren, Claudia
Thomalla, Götz
von dem Knesebeck, Olaf
Waschki, Benjamin
Wegscheider, Karl

Zeller, Tanja
Zyriax, Birgit-Christiane

Steering Board:
Augustin, Matthias
Blankenberg, Stefan
Gallinat, Jürgen
Gerloff, Christian
Härter, Martin
Jagodzinski, Annika
Johansen, Christoffer
Koch-Gromus, Uwe
Sauter, Guido
Zeller, Tanja
Wegscheider, Karl
Betz, Christian/ Heydecke, Guido/ Gosau, Martin

Research consortium:
Aarabi, Ghazal
Andrees, Valerie
Behrendt, Christian Brassen, Stefanie
Brekenfeld, Caspar
Brünahl, Christian
Busch, Chia-Jung
Freitag, Janina
Gallinat, Jürgen
Gellißen, Susanne
Girdauskas, Evaldas
Heidemann, Christoph
Hussein, Yassin
Klein, Verena
Kofahl, Christopher
Kohlmann, Sebastian
Konnopka, Alexander

Kühn, Simone
Lühmann, Dagmar
Lund, Gunnar
Magnussen, Christina
Meyer, Christian
Nagel, Lina
Petersen, Elina
Scherschel, Katharina
Schiffner, Ulrich
Schnabel, Renate
Schulz, Holger
Seedorf, Udo
Smeets, Ralf
Terschüren, Claudia
Thomalla, Götz
Waschki, Benjamin
Zeller, Tanja
Zyriax, Birgit-Christiane

Study Funding
The participating institutes and departments from the University Medical Center Hamburg-Eppendorf contribute all with individual and scaled budgets to the overall funding. The Hamburg City Health Study is also supported by Amgen, Astra Zeneca, Bayer, BASF, Deutsche Gesetzliche Unfallversicherung (DGUV), DIFE, the Innovative medicine initiative (IMI) under grant number No. 116074 and the Fondation Leducq under grant number 16 CVD 03., Novartis, Pfizer, Schiller, Siemens, Unilever and "Förderverein zur Förderung der HCHS e.V.".
This work was supported by the Deutsche Forschungsgemeinschaft
(DFG), Sonderforschungsbereich (SFB) 936, Project C1 (C. Gerloff), Project C2 (J. Fiehler, G. Thomalla, B.Cheng).

Data Availability Statement

Due to the nature of this research, participants of this study did not agree for their data to be shared publicly, so supporting data is not available.

References:

Alexopoulos GS (2006): The Vascular Depression Hypothesis: 10 Years Later. Biol Psychiatry 60:1304–1305. https://linkinghub.elsevier.com/retrieve/pii/S0006322306011103.

Andersson JLR, Sotiropoulos SN (2016): An integrated approach to correction for off-resonance effects and subject movement in diffusion MR imaging. Neuroimage 125:1063–1078. http://www.ncbi.nlm.nih.gov/pubmed/26481672.

Aparicio HJ, Petrea RE, Massaro JM, Manning WJ, Oyama-Manabe N, Beiser AS, Kase CS, D'Agostino RB, Wolf PA, Vasan RS, DeCarli C, O'Donnell CJ, Seshadri S (2017): Association of descending thoracic aortic plaque with brain atrophy and white matter hyperintensities: The Framingham Heart Study. Atherosclerosis 265:305–311.

Avants B, Epstein C, Grossman M, Gee J (2008): Symmetric diffeomorphic image registration with cross-correlation: Evaluating automated labeling of elderly and neurodegenerative brain. Med Image Anal 12:26–41. https://linkinghub.elsevier.com/retrieve/pii/S1361841507000606.

Bassett DS, Bullmore ET, Meyer-Lindenberg A, Apud JA, Weinberger DR, Coppola R (2009): Cognitive fitness of cost-efficient brain functional networks. Proc Natl Acad Sci 106:11747–11752. http://www.ncbi.nlm.nih.gov/pubmed/19564605.

Baykara E, Gesierich B, Adam R, Tuladhar AM, Biesbroek JM, Koek HL, Ropele S, Jouvent E, Chabriat H, Ertl-Wagner B, Ewers M, Schmidt R, de Leeuw F-E, Biessels GJ, Dichgans M, Duering M, Duering M (2016): A Novel Imaging Marker for Small Vessel Disease Based on Skeletonization of White Matter Tracts and Diffusion Histograms. Ann Neurol 80:581–592. http://doi.wiley.com/10.1002/ana.24758.

Berlot R, Metzler-Baddeley C, Ikram MA, Jones DK, O'Sullivan MJ (2016): Global Efficiency of Structural Networks Mediates Cognitive Control in Mild Cognitive Impairment. Front Aging Neurosci 8:292. http://www.ncbi.nlm.nih.gov/pubmed/28018208.

Brodal P (2016): The Central Nervous System. Oxford University Press. http://oxfordmedicine.com/view/10.1093/med/9780190228958.001.0001/med-9780190228958.

Cees De Groot J, De Leeuw F-E, Oudkerk M, Van Gijn J, Hofman A, Jolles J, Breteler MMB (2000): Cerebral white matter lesions and cognitive function: The Rotterdam scan study. Ann Neurol 47:145–151. http://doi.wiley.com/10.1002/1531-

8249%28200002%2947%3A2%3C145%3A%3AAID-ANA3%3E3.0.CO%3B2-P.

Civier O, Smith RE, Yeh C-H, Connelly A, Calamante F (2019): Is removal of weak connections necessary for graph-theoretical analysis of dense weighted structural connectomes from diffusion MRI? Neuroimage 194:68–81. https://www.sciencedirect.com/science/article/pii/S1053811919301351.

Costa L da F, Oliveira ON, Travieso G, Rodrigues FA, Villas Boas PR, Antiqueira L, Viana MP, Correa Rocha LE (2011): Analyzing and modeling real-world phenomena with complex networks: a survey of applications. Adv Phys 60:329–412. http://www.tandfonline.com/doi/abs/10.1080/00018732.2011.572452.

Crofts JJ, Higham DJ, Bosnell R, Jbabdi S, Matthews PM, Behrens TEJ, Johansen-Berg H (2011): Network analysis detects changes in the contralesional hemisphere following stroke. Neuroimage 54:161–169. https://www.sciencedirect.com/science/article/pii/S1053811910011146.

Dancause N, Barbay S, Frost SB, Plautz EJ, Chen D, Zoubina E V., Stowe AM, Nudo RJ (2005): Journal of Neuroscience. J Neurosci 24:1200–1211.

DeCarli C, Fletcher E, Ramey V, Harvey D, Jagust WJ (2005): Anatomical Mapping of White Matter Hyperintensities (WMH). Stroke 36:50–55. https://www.ahajournals.org/doi/10.1161/01.STR.0000150668.58689.f2.

Desikan RS, Segonne F, ́Fischl B, Quinn BT, Dickerson BC, Blacker D, Buckner RL, Dale AM, Maguire RP, Hyman BT, Albert MS, Killiany and RJ (2006): An automated labeling system for subdividing the human cerebral cortex on MRI scans into gyral based regions of interest.

Diedenhofen B, Musch J (2015): cocor: a comprehensive solution for the statistical comparison of correlations. PLoS One 10:e0121945. http://www.ncbi.nlm.nih.gov/pubmed/25835001.

Duering M, Finsterwalder S, Baykara E, Tuladhar AM, Gesierich B, Konieczny MJ, Malik R, Franzmeier N, Ewers M, Jouvent E, Biessels GJ, Schmidt R, de Leeuw F-E, Pasternak O, Dichgans M (2018): Free water determines diffusion alterations and clinical status in cerebral small vessel disease. Alzheimer's Dement 14:764–774. https://www.sciencedirect.com/science/article/abs/pii/S1552526018300013?via%3Dihub.

Filipek PA, Richelme C, Kennedy DN, Caviness VS (1994): The young adult human brain: An MRI-based morphometric analysis. Cereb Cortex 4:344–360. https://pubmed.ncbi.nlm.nih.gov/7950308/.

Fornito A, Bullmore ET (2015): Connectomics : A new paradigm for understanding brain disease:733–748.

Frey BM, Petersen M, Mayer C, Schulz M, Cheng B, Thomalla G (2019): Characterization of

White Matter Hyperintensities in Large-Scale MRI-Studies. Front Neurol 10:238. https://www.frontiersin.org/article/10.3389/fneur.2019.00238/full.

Griffanti L, Jenkinson M, Suri S, Zsoldos E, Mahmood A, Filippini N, Sexton CE, Topiwala A, Allan C, Kivimäki M, Singh-Manoux A, Ebmeier KP, Mackay CE, Zamboni G (2018): Classification and characterization of periventricular and deep white matter hyperintensities on MRI: A study in older adults. Neuroimage 170:174–181. https://www.sciencedirect.com/science/article/pii/S1053811917302318?via%3Dihub.

Griffanti L, Zamboni G, Khan A, Li L, Bonifacio G, Sundaresan V, Schulz UG, Kuker W, Battaglini M, Rothwell PM, Jenkinson M (2016): BIANCA (Brain Intensity AbNormality Classification Algorithm): A new tool for automated segmentation of white matter hyperintensities. Neuroimage 141:191–205. http://www.ncbi.nlm.nih.gov/pubmed/27402600.

Heuvel MP van den, Stam CJ, Kahn RS, Pol HEH (2009): Efficiency of Functional Brain Networks and Intellectual Performance. J Neurosci 29:7619–7624. http://www.jneurosci.org/content/29/23/7619.long.

Jagodzinski A, Johansen C, Koch-Gromus U, Aarabi G, Adam G, Anders S, Augustin M, der Kellen RB, Beikler T, Behrendt CA, Betz CS, Bokemeyer C, Borof K, Briken P, Busch CJ, Büchel C, Brassen S, Debus ES, Eggers L, Fiehler J, Gallinat J, Gellißen S, Gerloff C, Girdauskas E, Gosau M, Graefen M, Härter M, Harth V, Heidemann C, Heydecke G, Huber TB, Hussein Y, Kampf MO, von dem Knesebeck O, Konnopka A, König HH, Kromer R, Kubisch C, Kühn S, Loges S, Löwe B, Lund G, Meyer C, Nagel L, Nienhaus A, Pantel K, Petersen E, Püschel K, Reichenspurner H, Sauter G, Scherer M, Scherschel K, Schiffner U, Schnabel RB, Schulz H, Smeets R, Sokalskis V, Spitzer MS, Terschüren C, Thederan I, Thoma T, Thomalla G, Waschki B, Wegscheider K, Wenzel JP, Wiese S, Zyriax BC, Zeller T, Blankenberg S (2019): Rationale and Design of the Hamburg City Health Study. Eur J Epidemiol.

Kellner E, Dhital B, Kiselev VG, Reisert M (2016): Gibbs-ringing artifact removal based on local subvoxel-shifts. Magn Reson Med 76:1574–1581. http://doi.wiley.com/10.1002/mrm.26054.

Latora V, Marchiori M (2001): Efficient Behavior of Small-World Networks. Phys Rev Lett 87:198701. https://link.aps.org/doi/10.1103/PhysRevLett.87.198701.

Lawrence AJ, Chung AW, Morris RG, Markus HS, Barrick TR (2014): Structural network efficiency is associated with cognitive impairment in small-vessel disease. Neurology 83:304. http://www.ncbi.nlm.nih.gov/pubmed/24951477.

Li Y, Liu Y, Li J, Qin W, Li K, Yu C, Jiang T (2009): Brain Anatomical Network and Intelligence. Ed. Olaf Sporns. PLoS Comput Biol 5:e1000395. http://dx.plos.org/10.1371/journal.pcbi.1000395.

Markov NT, Misery P, Falchier A, Lamy C, Vezoli J, Quilodran R, Gariel MA, Giroud P, Ercsey-Ravasz M, Pilaz LJ, Huissoud C, Barone P, Dehay C, Toroczkai Z, Van Essen DC, Kennedy H, Knoblauch K (2011): Weight Consistency Specifies Regularities of Macaque Cortical Networks. Cereb Cortex 21:1254–1272. https://academic.oup.com/cercor/article-lookup/doi/10.1093/cercor/bhq201.

Maslov S, Sneppen K, Zaliznyak A (2002): Pattern Detection in Complex Networks: Correlation Profile of the Internet. http://arxiv.org/abs/cond-mat/0205379.

Muldoon SF, Bridgeford EW, Bassett DS (2016): Small-world propensity and weighted brain networks. Sci Rep 6:1–13. www.nature.com/scientificreports/.

Newman MEJ (2006): Modularity and community structure in networks. http://arxiv.org/abs/physics/0602124.

van Norden AGW, van Uden IWM, de Laat KF, van Dijk EJ, de Leeuw F-E (2012): Cognitive Function in Small Vessel Disease: The Additional Value of Diffusion Tensor Imaging to Conventional Magnetic Resonance Imaging: The RUN DMC Study. Ed. Jack de la Torre. J Alzheimer's Dis 32:667–676. http://www.medra.org/servlet/aliasResolver?alias=iospress&doi=10.3233/JAD-2012-120784.

Onnela J-P, Saramäki J, Kertész J, Kaski K (2005): Intensity and coherence of motifs in weighted complex networks. Phys Rev E 71:065103. http://www.ncbi.nlm.nih.gov/pubmed/16089800.

Pantoni L (2010): Cerebral small vessel disease: from pathogenesis and clinical characteristics to therapeutic challenges. Lancet Neurol 9:689–701. https://www.sciencedirect.com/science/article/pii/S1474442210701046?via%3Dihub.

Petersen M, Frey BM, Schlemm E, Mayer C, Hanning U, Engelke K, Fiehler J, Borof K, Jagodzinski A, Gerloff C, Thomalla G, Cheng B (2020): Network Localisation of White Matter Damage in Cerebral Small Vessel Disease. Sci Rep 10:1–9. https://www.nature.com/articles/s41598-020-66013-w.

Reijmer YD, Fotiadis P, Martinez-Ramirez S, Salat DH, Schultz A, Shoamanesh A, Ayres AM, Vashkevich A, Rosas D, Schwab K, Leemans A, Biessels G-J, Rosand J, Johnson KA, Viswanathan A, Gurol ME, Greenberg SM (2015): Structural network alterations and neurological dysfunction in cerebral amyloid angiopathy. Brain 138:179–188. https://academic.oup.com/brain/article-lookup/doi/10.1093/brain/awu316.

Rensma SP, van Sloten TT, Launer LJ, Stehouwer CDA (2018): Cerebral small vessel disease and risk of incident stroke, dementia and depression, and all-cause mortality: A systematic review and meta-analysis. Neurosci Biobehav Rev 90:164–173. https://www.sciencedirect.com/science/article/pii/S0149763417307777.

Roalf DR, Quarmley M, Elliott MA, Satterthwaite TD, Vandekar SN, Ruparel K, Gennatas

ED, Calkins ME, Moore TM, Hopson R, Prabhakaran K, Jackson CT, Verma R, Hakonarson H, Gur RC, Gur RE (2016): The impact of quality assurance assessment on diffusion tensor imaging outcomes in a large-scale population-based cohort. Neuroimage 125:903–919. http://www.ncbi.nlm.nih.gov/pubmed/26520775.

Rubinov M, Sporns O (2010): Complex network measures of brain connectivity: Uses and interpretations. Neuroimage 52:1059–1069. https://www.sciencedirect.com/science/article/pii/S105381190901074X?via%3Dihub.

Smith RE, Tournier J-D, Calamante F, Connelly A (2012): Anatomically-constrained tractography: Improved diffusion MRI streamlines tractography through effective use of anatomical information. Neuroimage 62:1924–1938. http://www.ncbi.nlm.nih.gov/pubmed/22705374.

Smith RE, Tournier J-D, Calamante F, Connelly A (2015): The effects of SIFT on the reproducibility and biological accuracy of the structural connectome. Neuroimage 104:253–265. https://www.sciencedirect.com/science/article/pii/S1053811914008155?via%3Dihub.

Smith SM, Jenkinson M, Johansen-Berg H, Rueckert D, Nichols TE, Mackay CE, Watkins KE, Ciccarelli O, Cader MZ, Matthews PM, Behrens TEJ (2006): Tract-based spatial statistics: Voxelwise analysis of multi-subject diffusion data. Neuroimage 31:1487–1505. https://www.sciencedirect.com/science/article/pii/S1053811906001388?via%3Dihub.

Sporns O, Zwi JD (2004): The Small World of the Cerebral Cortex. Neuroinformatics 2:145–162. http://link.springer.com/10.1385/NI:2:2:145.

Stam CJ (2014): Modern network science of neurological disorders. Nat Rev Neurosci 15:683–695. http://www.nature.com/doifinder/10.1038/nrn3801.

Stellmann J-P, Hodecker S, Cheng B, Wanke N, Young KL, Hilgetag C, Gerloff C, Heesen C, Thomalla G, Siemonsen S (2017): Reduced rich-club connectivity is related to disability in primary progressive MS. Neurol - Neuroimmunol Neuroinflammation 4:e375. http://nn.neurology.org/lookup/doi/10.1212/NXI.0000000000000375.

ter Telgte A, van Leijsen EMC, Wiegertjes K, Klijn CJM, Tuladhar AM, de Leeuw F-E (2018): Cerebral small vessel disease: from a focal to a global perspective. Nat Rev Neurol 14:387–398. http://www.nature.com/articles/s41582-018-0014-y.

Tournier, J.-D. Calamante, F. & Connelly A (2010): Improved probabilistic streamlines tractography by 2nd order integration over fibre orientation distributions. Proc Int Soc Magn Reson Med:1670.

Tournier J-D, Smith RE, Raffelt DA, Tabbara R, Dhollander T, Pietsch M, Christiaens D, Jeurissen B, Yeh C-H, Connelly A (2019): MRtrix3: A fast, flexible and open software framework for medical image processing and visualisation. bioRxiv:551739.

https://www.biorxiv.org/content/10.1101/551739v1.

Tuladhar AM, van Dijk E, Zwiers MP, van Norden AGW, de Laat KF, Shumskaya E, Norris DG, de Leeuw F-E, Dijk E van, Zwiers MP, Norden AGW van, Laat KF de, Shumskaya E, Norris DG, Leeuw F de, van Dijk E, Zwiers MP, van Norden AGW, de Laat KF, Shumskaya E, Norris DG, de Leeuw F-E (2016a): Structural network connectivity and cognition in cerebral small vessel disease. Hum Brain Mapp 37:300–310. http://doi.wiley.com/10.1002/hbm.23032.

Tuladhar AM, van Uden IWM, Rutten-Jacobs LCA, Lawrence A, van der Holst H, van Norden A, de Laat K, van Dijk E, Claassen JAHR, Kessels RPC, Markus HS, Norris DG, de Leeuw F-E (2016b): Structural network efficiency predicts conversion to dementia. Neurology 86:1112–9. http://www.ncbi.nlm.nih.gov/pubmed/26888983.

Tustison NJ, Avants BB, Cook PA, Yuanjie Zheng, Egan A, Yushkevich PA, Gee JC (2010): N4ITK: Improved N3 Bias Correction. IEEE Trans Med Imaging 29:1310–1320. http://ieeexplore.ieee.org/document/5445030/.

Veraart J, Novikov DS, Christiaens D, Ades-aron B, Sijbers J, Fieremans E (2016): Denoising of diffusion MRI using random matrix theory. Neuroimage 142:394–406. http://www.ncbi.nlm.nih.gov/pubmed/27523449.

Wardlaw JM, Smith EE, Biessels GJ, Cordonnier C, Fazekas F, Frayne R, Lindley RI, O'Brien JT, Barkhof F, Benavente OR, Black SE, Brayne C, Breteler M, Chabriat H, DeCarli C, de Leeuw F-E, Doubal F, Duering M, Fox NC, Greenberg S, Hachinski V, Kilimann I, Mok V, Oostenbrugge R van, Pantoni L, Speck O, Stephan BCM, Teipel S, Viswanathan A, Werring D, Chen C, Smith C, van Buchem M, Norrving B, Gorelick PB, Dichgans M (2013): Neuroimaging standards for research into small vessel disease and its contribution to ageing and neurodegeneration. Lancet Neurol 12:822–838.

Watts DJ, Strogatz SH (1998): Collective dynamics of 'small-world' networks. Nature 393:440–442. http://www.nature.com/articles/30918.

Wei N, Deng Y, Yao L, Jia W, Wang J, Shi Q, Chen H, Pan Y, Yan H, Zhang Y, Wang Y (2019): A Neuroimaging Marker Based on Diffusion Tensor Imaging and Cognitive Impairment Due to Cerebral White Matter Lesions. Front Neurol 10:81. https://www.frontiersin.org/article/10.3389/fneur.2019.00081/full.

Xie X, Shi Y, Zhang J (2017): Structural network connectivity impairment and depressive symptoms in cerebral small vessel disease. J Affect Disord 220:8–14. https://www.sciencedirect.com/science/article/pii/S0165032717305682?via%3Dihub.

Box, table and figures:

Weighted clustering coefficient [Onnela et al., 2005; Watts and Strogatz, 1998] The weighted clustering coefficient of a node is defined as the normalised sum of geometrically averaged edge weights of all triangles associated with the node. Thus, the average of this parameter over all nodes indicates how intensively the network is locally interconnected and thereby reflects its capability of segregated computation.
Modularity Q [Newman, 2006] The modularity Q is the result of an iterative optimization process. First, partition of the connectome in nonoverlapping modules - i.e. highly interconnected subgroups of nodes - is performed by applying Newman's spectral community detection. Upon that the modularity Q is calculated: for each module the weighted count of edges present within the module is surveyed and subtracted by the weighted edge count expected by chance. Subsequently, all module specific values are summed up resulting in Q. Hence, a positive Q indicates a higher intramodular connectivity than expected by chance, indicating modular structure. Based on the former partition a new partition is defined by an optimization algorithm and this process is reiterated until Q doesn't increase anymore. This maximal Q is the value reported.
Weighted global efficiency [Latora and Marchiori, 2001] The global efficiency is defined as the average inverse shortest path length. The length of a path between two nodes is the total weight of edges comprising that path.
Small-world propensity {Muldoon et al., 2016} The small-world propensity allows for quantification of small-world structure in weighted and dense networks: it indicates how much a networks clustering coefficient and shortest path length deviate from random and lattice null models with the same node amount and degree distribution and relates both deviations. Thus, the parameter provides insights about the degree a network exhibits parallel presence of strong integration and segregation characteristics. A network with a small-world propensity above 0.6 is considered to show pronounced small-world structure.

Box 1: Global graph parameters derived in this study

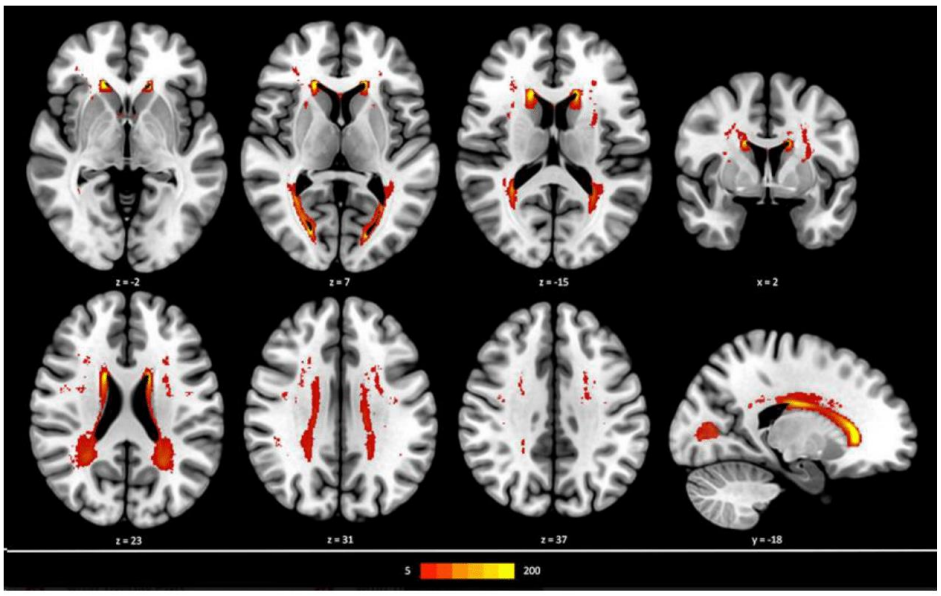

Figure 1: *Distribution of White Matter Hyperintensities (WMH) in a cohort of 930 participants.* The map presents the frequency of WMH in a specific voxel as indicated by the coloured bar and superimposed on a standard brain template in MNI-152 space.

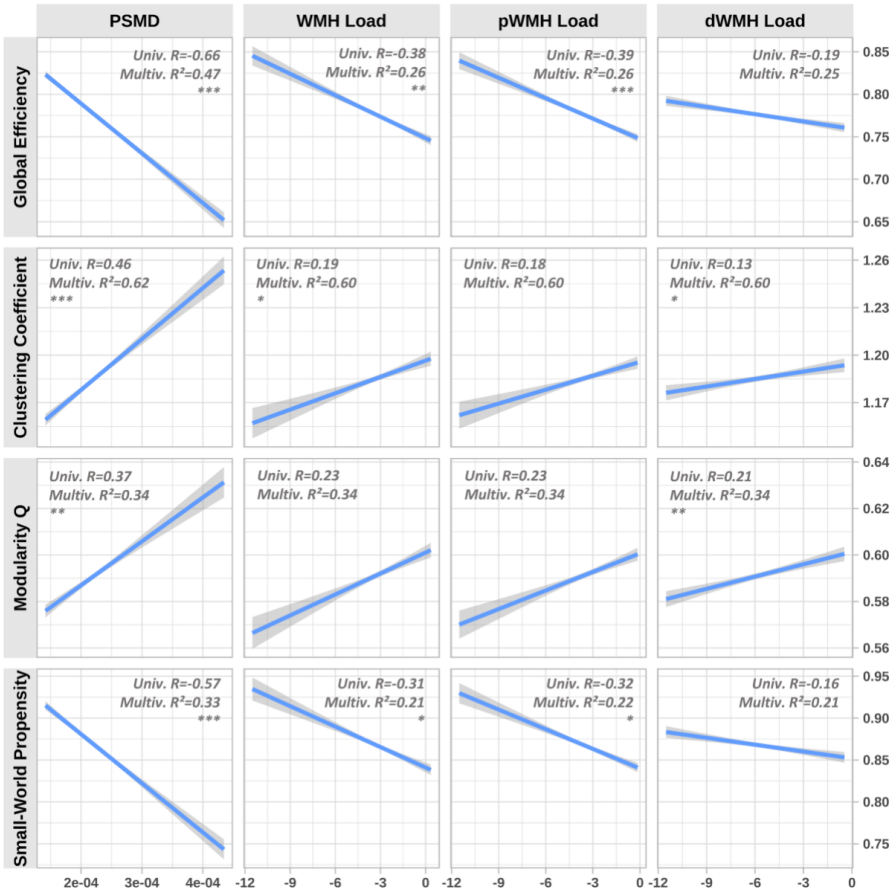

Figure 2: *Association of CSVD surrogate markers with global graph parameters*
Results of simple linear regression modelling are illustrated using CSVD surrogate markers as independent variables (columns) and global topological graph parameters as dependent variables (rows). Gray bands represent confidence intervals. Correlation (R) from simple correlation analysis and explained variance (R^2) from multivariable models are reported. Asterisks indicate level of significance after inclusion of covariates (*=p<0.05, **=p<0.01, ***=p<0.001). PSMD = peak width of skeletonised mean diffusivity, WMH = total White Matter Hyperintensities, pWMH = periventricular White Matter Hyperintensities, dWMH = deep White Matter Hyperintensities.

Variable	Count
Sex = female	424 (45.6%)
Age [years], median (IQR)	64 (14)
Vascular risk factors	
History of smoking, n (%)	560 (66.1%)
History of hypertension, n (%)	637 (72.0%)
Diabetes, n (%)	74 (8.7%)
Body-Mass-Index, median (IQR)	26.2 (5.5)
Conventional MRI measures	
Brain volume [ml], median (IQR)	1483.7 (203.1)
Ventricle volume [ml], median (IQR)	25.4 (18.4)
WMH volume [ml], median (IQR)	0.6 (1.4)
pWMH volume [ml], median (IQR)	0.5 (1.1)
dWMH volume [ml], median (IQR)	0.1 (0.2)
WMH load [%], median (IQR)	0.04 (0.09)
pWMH load [%], median (IQR)	0.03 (0.08)
dWMH load [%], median (IQR)	0.01 (0.01)
PSMD [mm2/s x 10^{-4}], median (IQR)	2.18 (0.5)
Graph theoretical network measures	
Edge Strength, median (IQR)	28.1 (9.5)
Network density, median (IQR)	0.880 (0.030)
Norm. global efficiency, median (IQR)	0.780 (0.045)
Standard error for null model global efficiency, median (IQR)	0.001 (<0.001)
Norm. clustering coefficient, median (IQR)	1.182 (0.034)
Standard error for null model clustering coefficient, median (IQR)	<0.001 (<0.001)
Modularity Q, median (IQR)	0.593 (0.026)

Small-world Propensity, median (IQR)	0.876 (0.040)

Table 1: characteristics of the study sample

PSMD = peak width of skeletonised mean diffusivity, WMH = total White Matter Hyperintensities, pWMH = periventricular White Matter Hyperintensities, dWMH = deep White Matter Hyperintensities, Norm. = normalised

Data was partly unavailable for the following variables (n): History of smoking (83), History of hypertension (45), Diabetes (80), Body-Mass-Index (56)

Acceptance Letter

HBM-20-0335.R2, Accept Manuscript, Human Brain Mapping.

Simon Eickhoff <onbehalfof@manuscriptcentral.com> 16. November 2020 um 22:11
Antwort an: simon.b.eickhoff@gmail.com
An: b.frey@uke.de, marvinpetersen94@gmail.com, e.schlemm@uke.de, c.mayer@uke.de, u.hanning@uke.de, k.radelfahr@uke.de, fiehler@uke.de, k.borof@uke.de, a.jagodzinski@uke.de, gerloff@uke.de, thomalla@uke.de, b.cheng@uke.de

Date:16-Nov-2020

Dear Mr. Frey:

RE: HBM-20-0335.R2, White matter integrity and structural brain network topology in cerebral small vessel disease - the Hamburg City Health Study

I am pleased to inform you that your manuscript has been reviewed and accepted for publication in Human Brain Mapping.

If all of your final accepted files have NOT been submitted in either .doc or .rtf format for the text/tables and either .tif or .eps format for the figures, you may receive a request to provide new files.

The final version of your article cannot be published until the publisher has received the appropriate signed license agreement. Once your article has been received by Wiley for production the corresponding author will receive an email from Wiley's Author Services system which will ask them to log in and will present them with the appropriate license for completion.

Payment of your Open Access Article Publication Charge (APC):
All articles published in Human Brain Mapping are fully open access: immediately and freely available to read, download and share. Human Brain Mapping charges an article publication charge (APC).

Before we can publish your article, your payment must be completed. The corresponding author for this manuscript will have already received a quote email shortly after original submission with the estimated Article Publication Charge; please let us know if this has not been received. Once your accepted paper is in production, the corresponding author will receive an e-mail inviting them to register with or log in to Wiley Author Services (www.wileyauthors.com) where the publication fee can be paid by credit card, or an invoice or proforma can be requested. The option to pay via credit card and claim reimbursement from your institution may help to avoid delays with payment processing.

You may contact Rebecca Strauss if you have any questions about this process at hbm@wiley.com

If you wish to submit artwork to be considered for the cover of the issue in which your article will appear, please contact hbmeic@uthscsa.edu for instructions.

To ensure that your digital graphics are suitable for print purposes, please go to RapidInspector™ at http://rapidinspector.cadmus.com/wi/index.jsp. This free, stand-alone software application will help you to inspect and verify illustrations right on your computer.

Thank you for your support of Human Brain Mapping. I look forward to seeing more of your work in the future.

Sincerely,

Dr. Simon Eickhoff
Editor-in-Chief, Human Brain Mappingsimon.b.eickhoff@gmail.com

P.S. – You can help your research get the attention it deserves! Wiley Editing Services offers professional video abstract and infographic creation to help you promote your research at www.wileyauthors.com/eeo/promotion. And, check out Wiley's free Promotion Guide for best-practice recommendations for promoting your work at www.wileyauthors.com/eeo/guide.

3 Darstellung der Publikationen mit Literaturverzeichnis

Hintergrund

Diese Arbeit basiert auf zwei Veröffentlichungen (Frey et al., n.d.; Petersen et al., 2020) und behandelt die Auswirkungen der cerebralen Mikroangiopathie (engl. cerebral small vessel disease, CSVD) auf die Hirnnetzwerktopologie. Der CSVD liegt eine altersassoziierte pathologische Veränderung der kleinkalibrigen perforierenden cerebralen Gefäße zugrunde (Pantoni, 2010). Klinisch charakterisiert durch ein substantiell erhöhtes Schlaganfall- und Demenzrisiko, ist sie von hoher sozioökonomischer Bedeutsamkeit in den Industrienationen (Debette and Markus, 2010; Rensma et al., 2018). Weiterhin manifestiert sich die Erkrankung klinisch durch kognitive Einschränkungen, Depression und Gangauffälligkeiten (de Laat et al., 2010; Frey et al., 2019; van Agtmaal et al., 2017; van der Holst et al., 2018). Diese Assoziation von Klinik und Pathologie der CSVD ist weitgehend ungeklärt und Gegenstand aktueller Untersuchungen.

Moderne Methodiken der Hirnbildgebung – besonders die Magnetresonanztomographie (MRT) – erlauben die Untersuchung der CSVD in-vivo und leisten einen großen Beitrag zur Aufklärung der Pathophysiologie. Typische Manifestationen der Erkrankung in der MRT sind T2-Hyperintensitäten der weißen Substanz vaskulärer Ursache (engl. white matter hyperintensities of presumed vascular origin, WMH), Atrophie, vergrößerte perivaskuläre Räume und cerebrale Mikroblutungen (Wardlaw et al., 2013). Vor allem MR-Diffusionsbildgebung (engl. Diffusion-weighted imaging, DWI) scheint geeignet um CSVD-induzierte Effekte auf die Integrität der weißen Substanz zu detektieren. So zeigten mehrere Studien charakteristische Veränderungen in Diffusions-Tensor-Bildgebung-basierten (DTI) Metriken, welche sensitiv für mikrostrukturelle Hirnparenchymveränderungen sind. Diese wiesen auf einen Faserverlust und erhöhte isotrope Wassermobilität in WMH und der periläsionalen weißen Substanz hin (de Groot et al., 2013; Maillard et al., 2013). In diffusionsgewichteten Bildern codiert sind neben mikrostrukturellen Informationen auch solche der Faserverläufe der weißen Substanz. Auf Basis dieser Informationen ist die Rekonstruktion struktureller Konnektome möglich. Strukturelle Konnektome sind approximative Repräsentationen des menschlichen Hirnnetzwerks, die sich aus Knoten und diese

verbindende Kanten zusammensetzen. Die Knoten repräsentieren hier Subareale der grauen Substanz und Kanten durch Traktographie rekonstruierte Faserbündel der weißen Substanz. Unter Anwendung netzwerkanalytischer Methoden, erlauben sie eine Charakterisierung topologischer Aspekte einer Krankheit. Wie bei anderen Hirnerkrankungen ist im Falle der CSVD eine Assoziation von primärer Gefäßpathologie und klinischer Symptomatik durch netzwerktopologische Krankheitsaspekte anzunehmen. Folglich wurde diese Analyse mit dem Ziel der Charakterisierung von CSVD-induzierten netzwerktopologischen Veränderungen durchgeführt.

Methodik

Die untersuchten Daten sind Bestandteil der Hamburg City Health Study (HCHS) – einer prospektiven und populationsbasierten Kohortenstudie. Bei den untersuchten Probanden handelt es sich um die Subgruppe der ersten 1000 Teilnehmern mit kardiovaskulärem Risikoprofil.

Die Quantifikation der CSVD-Belastung erfolgte durch Berechnung der peak-width of skeletonised mean diffusivity (PSMD) und der WMH-Last (WMH load). Die PSMD ist eine auf DTI basierende Metrik, deren Berechnung robust ist und die in ausgeprägtem Maße mit klinischen Symptomen der CSVD korreliert (Baykara et al., 2016). Für die WMH-Last wurde das WMH Volumen automatisiert quantifiziert (Griffanti et al., 2016) und ins Verhältnis zum intrakraniellen Volumen gesetzt. Zudem wurden die Läsionen gemäß der Distanz zu den Ventrikeln in periventrikuläre und tiefe WMH unterteilt.

Die Rekonstruktion der strukturellen Hirnnetzwerke basiert auf T1- und diffusionsgewichteter MR-Bildgebung. Mittels FreeSurfer wurde die graue Substanz gemäß dem Desikan-Killiany-Atlas in 84 Areale parcelliert, welche die Netzwerkknoten definierten (Desikan et al., 2006). Probabilistisch traktographiert wurde unter Anwendung von in Mrtrix3 implementierten Methodiken wie Constrained spherical deconvolution (CSD) sowie Spherical deconvolution-derived filtering of tractograms (SIFT2) (Smith et al., 2015; Tournier et al., 2004). Zwei Knoten wurden von einer Kante verbunden, falls Streamlines zwischen beiden

Knoten verliefen. Jeder Kante wurde ein Konnektivitätswert zugeordnet, der der gewichteten Anzahl der ihr zugrundeliegenden Streamlines entsprach.

Um zu untersuchen, welche Netzwerksektionen bevorzugt CSVD-induzierte Effekte aufweisen, wurden Kanten gemäß zweier Schemata unterteilt. 1) Entsprechend der verbundenen Areale der grauen Substanz in frontale, parietale, okzipitale, limbische, insuläre und subcortikale Areale assoziierende Kanten. 2) Entsprechend Kantenlänge und Verlauf in kurze intrahemisphärische, lange intrahemisphärische und interhemisphärische Kanten. Die Summe der Konnektivitätswerte einer Kantengruppe wurde berechnet, um einen repräsentativen Konnektivitätswert pro Faserbündelpopulation, pro Proband zu erhalten. Aufgrund der Anwendung von CSD erlaubt dieser Konnektivitätswert Rückschlüsse auf die tatsächliche mikrostrukturelle Faserarchitektur. Er entspricht nach Anwendung der Faserdichte der dem Diffusionssignal zugrundeliegenden realen Fasern der weißen Substanz. Ebenso wurde die relative Konnektivität berechnet, die dem Quotienten aus Konnektivität einer Kantengruppe und der Gesamtkonnektivität entspricht.

Die Berechnung von topologischen Netzwerkparametern erlaubte die Untersuchung der Assoziation von CSVD mit Veränderungen der globalen Netzwerktopologie. Dabei handelt es sich um Parameter, die Netzwerkcharakteristiken wie die Segregation (Clustering-Koeffizient, Modularität Q), Netzwerkintegration (Globale Effizienz) oder Small-worldness (Small-world propensity) zusammenfassen. Die Paramter wurden unter Anwendung der Brain connectivity toolbox (Rubinov and Sporns, 2010) berechnet.

Der Zusammenhang obiger Gruppenkonnektivitäten und topologischer Netzwerkparameter mit den CSVD-Surrogatmarkern wurde in linearen Modellen untersucht. Zudem wurden in einer explorativen klinischen Analyse die Assoziation der topologischen Netzwerkparameter sowie der CSVD-Surrogatmarker mit Ergebnissen des Mini-Mental-Status-Test (MMSE), trail making test a (TMT-A) sowie b (TMT-B) in linearen Modellen untersucht. Alter, Geschlecht, intrakranielles Volumen, mittleres Kantengewicht, cardiovaskuläre Risikofaktoren sowie Ausbildungsjahre sind aufgenommene Kovariaten. Die resultierenden p-Werte wurden nach Bonferroni korrigiert.

Resultate

Es wurden die Daten von 930 Teilnehmern statistisch ausgewertet, das heißt 70 Datensätze wurden im Rahmen der Qualitätsanalyse ausgeschlossen.

In den Analysen gemäß beider Unterteilungsschemata identifizierten die linearen Modelle Faserpopulationen deren Konnektivitätswerte nach Kovariateninklusion und Bonferroni-Korrektur signifikant mit der PSMD korrelierten. Um eine Untersuchung nach anatomisch vordefinierten Hirnarealen zu ermöglichen, wurden die Kanten in Gruppen entsprechend der verbundenen grauen Substanz unterteilt. Dabei zeigte die Konnektivität der Fasern signifikante negative Korrelationen mit der PSMD, die subcortikale, frontale, occipitale und parietale Areale verbanden. Die relative subcortikale und frontale Konnektivität waren signifikant negativ mit der PSMD korreliert. Die relative insuläre, temporale und cerebelläre Konnektivität korrelierten damit hingegen positiv.

Weiterhin wurden die Kanten gemäß des Verlaufs und der Länge der zugrundeliegenden Streamlines unterteilt. Die interhemisphärische, lange intrahemisphärische sowie kurze intrahemisphärische Konnektivität zeigten eine signifikant negative Assoziation mit der PSMD. Die relative interhemisphärische Konnektivität sowie die intrahemisphärischer und langer Kanten waren negativ mit der PSMD korreliert, wohingegen die relative Konnektivität kurzer intrahemisphärischer Kanten positiv korreliert war. Eine formale Interaktionsanalyse zeigte, dass alle untersuchten Assoziationen signifikant unterschiedlich waren.

Die PSMD zeigte signifikante negative Korrelationen mit der Globalen Effizienz und Small-world propensity und positive Korrelationen mit dem Clustering-Koeffizienten sowie der Modularität Q. Modelle mit der WMH-Last statt der PSMD als unabhängige Variable zeigten geringfügigere Effektgrößen und Signifikanzniveaus. Die Small-world propensity zeigte eine signifikante negative Assoziation mit dem TMT-A sowie -B. Die PSMD war nur mit dem TMT-B signifikant korreliert.

Diskussion

In dieser Untersuchung wurde in einem populationsbasierten Kollektiv bestehend aus 930 Probanden mit kardiovaskulären Risikofaktoren die Assoziation von cerebraler Mikroangiopathie mit mikrostrukturellen und netzwerktopologischen Veränderungen erhoben. Es ließ sich zeigen, dass bereits bei asymptomatischen Individuen mit geringfügiger WMH-Last CSVD-induzierte Konnektivitätsveränderungen nachweisbar sind und diese Veränderungen je nach Region unterschiedlich ausgeprägt waren. Subcorticale, frontale und occipitale sowie interhemisphärische und lange intrahemisphärische Kanten zeigten die deutlichsten negativen Korrelationen. Eine veränderte globale Netzwerktopologie – eine verringerte Small-world propensity sowie Globale Effizienz und erhöhte Segregationsparameter – gingen mit erhöhter CSVD-Belastung einher. Zudem waren CSVD-assoziierte mikrostrukturelle und netzwerktopologische Veränderungen mit schlechterer Testleistung im TMT assoziiert. Diese Ergebnisse leisten einen Beitrag zur weiteren Aufklärung der Pathophysiologie dieser Krankheit.

Wir konnten nachweisen, dass in einem relevanten Anteil der Netzwerkkanten eine verminderte Konnektivität mit erhöhten CSVD Markern einhergeht, was nach unserer Interpretation für eine Affektion eines großen Anteils der Faserpopulationen durch CSVD spricht. Dabei zeigten sich besonders lange und interhemisphärische Bündel durch CSVD geschädigt. Also Verbindungen, die aufgrund der Gewährleistung schnellen Informationstransfers zwischen entfernten Regionen sowie Kostspieligkeit in der Unterhaltung für das Gehirn einen besonderen Wert darstellen. Dieser Befund ist im Einklang mit vorherigen Untersuchungen (Lawrence et al., 2014; Tuladhar et al., 2017). Plausibel ist, dass lange callosale und assoziative Faserbündel primär periventrikulär und damit am Ort bevorzugten WMH-Aufkommens bei den hier untersuchten Probanden verlaufen. Zu beachten ist, dass diese Beobachtungen in einem populationsbasierten Teilnehmerkollektiv mit relativ geringer WMH Last gemacht wurden. Folglich kommt es selbst bei Individuen ohne sichtbare oder nur mit minimalen Läsionen in T2 zu hirnstrukturellen Veränderungen durch CSVD. Dies ist im Einklang mit vorherigen Untersuchungen, die zeigen, dass es jenseits der Grenzen von WMH zu charakteristischen mikrostrukturellen Veränderungen von DTI-Parametern kommt

sowie dass diese Veränderungen dem Auftreten von WMH vorangehen können (Maillard et al., 2014; Maniega et al., 2015; Wardlaw et al., 2015).

Darauf aufbauend führten wir eine komplexe Netzwerkanalyse durch, die eine Charakterisierung der Effekte von CSVD auf die globale Netzwerktopologie erlaubte. Laut früherer Untersuchungen liegt dem menschlichen Gehirn ein topologisches Organisationsparadigma genannt „Small-world“ zugrunde (Sporns and Zwi, 2004; Watts and Strogatz, 1998). Dieses beschreibt, dass die Architektur des Hirns einen funktionell optimalen Kompromiss aus ausgeprägter Segregation und Integration darstellt. Segregation beschreibt die Fähigkeit zur distribuierten Informationsverarbeitung und Integration die Eigenschaft diese distribuierten Prozesse sinnvoll zu vereinen. Die Integration ist nachweislich korreliert mit kognitiven Funktionen (Bassett et al., 2009; Van Den Heuvel et al., 2009). Unsere Arbeit demonstriert, dass erhöhte CSVD-Surrogatmarker mit erniedrigter Integration zugunsten einer hohen Segregation einhergehen. Diese Veränderungen ließen sich mit dem vorherigen Befund der beeinträchtigten langen und interhemisphärischen Bahnen erklären, da die zugrundeliegenden Netzwerkparameter von Präsenz beziehungsweise Fehlen entsprechender Kanten beeinflusst sind. Obendrein legt diese Veränderung eine Abweichung von der Small-world-Topologie nahe, die wir mit einer veränderten Small-world propensity nachweisen konnten.

Vaskuläre kognitive Beeinträchtigung (engl. vascular cognitive impairment; VCI) und vaskuläre Demenz zeichnen sich durch eine schwerwiegende klinische Symptomatik aus und können Folge der CSVD sein (Wallin et al., 2018). Wie genau kognitiven Symptomen und vaskulärer Pathologie im Falle dieser Erkrankungen assoziiert sind, ist jedoch weitgehend unverstanden. Die Netzwerkwissenschaften liefern Konzepte zur Überbrückung dieser Kluft. Von zentraler Bedeutung für die Fähigkeit des Hirns verteilte Informationen zusammenzuführen und zu integrieren sind Assoziations- und Kommissurenfasern. Entsprechend würde ein Verlust dieser Fasern mit einem eingeschränktem Informationsaustausch zwischen entfernt liegenden Hirnarealen einhergehen. Ergebnisse komplexer Netzwerkanalysen sprechen dafür, dass in CSVD-Patienten kognitive Leistungsfähigkeit wesentlich von dieser Integrationsfähigkeit abhängt (Lawrence et al., 2014). Damit im Einklang wurde gezeigt, dass Veränderungen von DTI Metriken im Corpus callosum und

langen Assoziationsfasern mit kognitiven Symptomen in CSVD einhergehen (Biesbroek et al., 2017; Tuladhar et al., 2015b). Weiterhin wird hypothetisiert, dass speziell die Affektion frontal-subcorticaler Netzwerke kognitive Symptome verursacht (Román et al., 2002). Dazu passt der Befund, dass frontale Atrophie im Rahmen der CSVD mit kognitiven Einschränkungen assoziiert ist (Tuladhar et al., 2015a). Unsere Ergebnisse zeigten, dass interhemisphärische und lange intrahemisphärische Faserpopulationen sowie solche die subcortikale oder frontale Hirnregionen verbinden bevorzugt von CSVD beeinträchtigt sind. Zudem zeigte sich in einer explorativen Analyse bei Teilnehmern mit verringerter Small-world propensity eine verringerte Testleistungsfähigkeit im TMT, was klinische Relevanz demonstriert. Damit erachten wir unsere Ergebnisse als gut vereinbar mit bestehender Literatur.

In der Zusammenschau legt diese Arbeit folgendes pathophysiologische Krankheitskonzept nahe: Bei CSVD führt ein vaskulärer Schaden zur Beeinträchtigung periventrikulär verlaufender langer und interhemisphärischer Fasertrakte. Dies geht mit einer Veränderung der globalen Netzwerktopologie einher. Eine verringerte Integration und erhöhte Segregation und damit ein Abweichen des Hirns von seiner ursprünglichen und als optimal angesehenen Organisationsstruktur hin zu einer eher distribuierten als integrierenden Informationsverarbeitung. Diese Abweichung von der Small-world-Topologie ist assoziiert mit klinischen Konsequenzen im Sinne eines verschlechterten kognitiven Funktion.

Stärken der vorgelegten Arbeit liegen in der Anwendung einer modernen und reproduzierbaren Bildverarbeitungspipeline sowie dem großen und hochwertigen Datensatz auf den sie angewendet wurde. Folgende Limitationen sind zu nennen. Zwar kardiovaskuläre Risiken aufweisend, handelt es sich beim untersuchten Kollektiv um asymptomatische Teilnehmer. Eine Untersuchung von Probanden mit fortgeschrittener sowie symptomatischer CSVD könnte weitere Aufschlüsse über die Pathophysiologie liefern. Ein longitudinales Studiendesign könnten wertvolle Einblicke in die strukturellen Netzwerkveränderungen über den Verlauf der CSVD liefern und somit Einblicke in Krankheitsdynamik gewähren. Weiterhin sind unsere Resultate vor dem Hintergrund der inhärenten Limitationen der Rekonstruktion

struktureller Konnektome zu interpretieren. So liegt der Traktographie ein vereinfachtes Diffusionsmodell (Tournier et al., 2004) zugrunde, der Anteil falsch-positiver Streamlines ist bei modernen Traktographieverfahren hoch (Maier-Hein et al., 2017) und die Erhebung netzwerktopologischer Parameter geht mit einer substantiellen Simplifizierung der Netzwerkcharakteristiken einher.

Weiterführende Ergebnisse

Da diese Arbeit zwar eine topologische, jedoch keine geometrische Einordnung der CSVD-induzierten Veränderungen zulässt, wurde ein noch unpubliziertes Folgeprojekt mit den Daten des selben Probandenkollektivs durchgeführt. Ein moderner auf Diffusionsbildgebung basierender Ansatz namens Fixel-basierte Analyse (FBA) erlaubte die Lokalisation von strukturellen Veränderungen der weißen Substanz im 3-dimensionalen Raum. Dabei handelt es sich um eine neue Methodik, die eine Untersuchung mikrostrukturelle Charakteristiken der weißen Substanz auf Subvoxel-Ebene, das heißt mehrerer Faserpopulationen pro Voxel, erlaubt. Die Ergebnisse der FBA weisen auf eine verringerte Faserdichte im Corpus callosum sowie langen intrahemisphärischen Trakten wie dem superioren longitudinalen Fasciculus hin. Zudem ließ sich nachweisen, dass eine verringerte Faserdichte und Atrophie in den benannten Trakten mit der Testleistung im TMT-A und -B korreliert. Insgesamt Ergebnisse, die mit der hier vorgelegten Arbeit gut vereinbar sind.

Literaturverzeichnis

Bassett, D.S., Bullmore, E.T., Meyer-Lindenberg, A., Apud, J.A., Weinberger, D.R., Coppola, R., 2009. Cognitive fitness of cost-efficient brain functional networks. Proceedings of the National Academy of Sciences of the United States of America 106, 11747–52. https://doi.org/10.1073/pnas.0903641106

Baykara, E., Gesierich, B., Adam, R., Tuladhar, A.M., Biesbroek, J.M., Koek, H.L., Ropele, S., Jouvent, E., Chabriat, H., Ertl-Wagner, B., Ewers, M., Schmidt, R., de Leeuw, F.-E., Biessels, G.J., Dichgans, M., Duering, M., Duering, M., 2016. A Novel Imaging Marker for Small Vessel Disease Based on Skeletonization of White Matter Tracts and Diffusion Histograms. Annals of Neurology 80, 581–592. https://doi.org/10.1002/ana.24758

Biesbroek, J.M., Leemans, A., den Bakker, H., Duering, M., Gesierich, B., Koek, H.L., van den Berg, E., Postma, A., Biessels, G.J., 2017. Microstructure of Strategic White Matter Tracts and Cognition in Memory Clinic Patients with Vascular Brain Injury. DEM 44, 268–282. https://doi.org/10.1159/000485376

de Groot, M., Verhaaren, B.F.J., de Boer, R., Klein, S., Hofman, A., van der Lugt, A., Ikram, M.A., Niessen, W.J., Vernooij, M.W., 2013. Changes in Normal-Appearing White Matter Precede Development of White Matter Lesions. Stroke 44, 1037–1042. https://doi.org/10.1161/STROKEAHA.112.680223

de Laat, K.F., van Norden, A.G.W., Gons, R.A.R., van Oudheusden, L.J.B., van Uden, I.W.M., Bloem, B.R., Zwiers, M.P., de Leeuw, F.-E., 2010. Gait in elderly with cerebral small vessel disease. Stroke 41, 1652–1658. https://doi.org/10.1161/STROKEAHA.110.583229

Debette, S., Markus, H.S., 2010. The clinical importance of white matter hyperintensities on brain magnetic resonance imaging: systematic review and meta-analysis. BMJ (Clinical research ed.) 341, c3666. https://doi.org/10.1136/bmj.c3666

Desikan, R.S., Segonne, F., ́Fischl, B., Quinn, B.T., Dickerson, B.C., Blacker, D., Buckner, R.L., Dale, A.M., Maguire, R.P., Hyman, B.T., Albert, M.S., Killiany, J, R., 2006. An automated labeling system for subdividing the human cerebral cortex on MRI scans into gyral based regions of interest.

Frey, B.M., Petersen, M., Mayer, C., Schulz, M., Cheng, B., Thomalla, G., 2019. Characterization of White Matter Hyperintensities in Large-Scale MRI-Studies. Front. Neurol. 10. https://doi.org/10.3389/fneur.2019.00238

Frey, B.M., Petersen, M., Schlemm, E., Mayer, C., Engelke, K., Fiehler, J., Borof, K., Jagodzinski, A., Gerloff, C., Thomalla, G., Cheng, B., n.d. White matter integrity and structural brain network topology in cerebral small vessel disease - the Hamburg City Health Study 30.

Griffanti, L., Zamboni, G., Khan, A., Li, L., Bonifacio, G., Sundaresan, V., Schulz, U.G., Kuker, W., Battaglini, M., Rothwell, P.M., Jenkinson, M., 2016. BIANCA (Brain Intensity AbNormality Classification Algorithm): A new tool for automated segmentation of white matter hyperintensities. NeuroImage 141, 191–205. https://doi.org/10.1016/j.neuroimage.2016.07.018

Lawrence, A.J., Chung, A.W., Morris, R.G., Markus, H.S., Barrick, T.R., 2014. Structural network efficiency is associated with cognitive impairment in small-vessel disease. Neurology 83, 304. https://doi.org/10.1212/WNL.0000000000000612

Maier-Hein, K.H., Neher, P.F., Houde, J.-C., Côté, M.-A., Garyfallidis, E., Zhong, J., Chamberland, M., Yeh, F.-C., Lin, Y.-C., Ji, Q., Reddick, W.E., Glass,

J.O., Chen, D.Q., Feng, Y., Gao, C., Wu, Y., Ma, J., He, R., Li, Q., Westin, C.-F., Deslauriers-Gauthier, S., González, J.O.O., Paquette, M., St-Jean, S., Girard, G., Rheault, F., Sidhu, J., Tax, C.M.W., Guo, F., Mesri, H.Y., Dávid, S., Froeling, M., Heemskerk, A.M., Leemans, A., Boré, A., Pinsard, B., Bedetti, C., Desrosiers, M., Brambati, S., Doyon, J., Sarica, A., Vasta, R., Cerasa, A., Quattrone, A., Yeatman, J., Khan, A.R., Hodges, W., Alexander, S., Romascano, D., Barakovic, M., Auría, A., Esteban, O., Lemkaddem, A., Thiran, J.-P., Cetingul, H.E., Odry, B.L., Mailhe, B., Nadar, M.S., Pizzagalli, F., Prasad, G., Villalon-Reina, J.E., Galvis, J., Thompson, P.M., Requejo, F.D.S., Laguna, P.L., Lacerda, L.M., Barrett, R., Dell'Acqua, F., Catani, M., Petit, L., Caruyer, E., Daducci, A., Dyrby, T.B., Holland-Letz, T., Hilgetag, C.C., Stieltjes, B., Descoteaux, M., 2017. The challenge of mapping the human connectome based on diffusion tractography. Nat Commun 8, 1–13. https://doi.org/10.1038/s41467-017-01285-x

Maillard, P., Carmichael, O., Harvey, D., Fletcher, E., Reed, B., Mungas, D., DeCarli, C., 2013. FLAIR and Diffusion MRI Signals Are Independent Predictors of White Matter Hyperintensities. AJNR Am J Neuroradiol 34, 54–61. https://doi.org/10.3174/ajnr.A3146

Maillard, P., Fletcher, E., Lockhart, S.N., Roach, A.E., Reed, B., Mungas, D., DeCarli, C., Carmichael, O., 2014. White Matter Hyperintensities and their Penumbra Lie Along a Continuum of Injury In The Aging Brain. Stroke 45, 1721–1726. https://doi.org/10.1161/STROKEAHA.113.004084

Maniega, S.M., Valdés Hernández, M.C., Clayden, J.D., Royle, N.A., Murray, C., Morris, Z., Aribisala, B.S., Gow, A.J., Starr, J.M., Bastin, M.E., Deary, I.J., Wardlaw, J.M., 2015. White matter hyperintensities and normal-appearing white matter integrity in the aging brain. Neurobiology of Aging 36, 909–918. https://doi.org/10.1016/j.neurobiolaging.2014.07.048

Pantoni, L., 2010. Cerebral small vessel disease: from pathogenesis and clinical characteristics to therapeutic challenges. The Lancet Neurology 9, 689–701. https://doi.org/10.1016/S1474-4422(10)70104-6

Petersen, M., Frey, B.M., Schlemm, E., Mayer, C., Hanning, U., Engelke, K., Fiehler, J., Borof, K., Jagodzinski, A., Gerloff, C., Thomalla, G., Cheng, B., 2020. Network Localisation of White Matter Damage in Cerebral Small Vessel Disease. Scientific Reports 10, 9210. https://doi.org/10.1038/s41598-020-66013-w

Rensma, S.P., van Sloten, T.T., Launer, L.J., Stehouwer, C.D.A., 2018. Cerebral small vessel disease and risk of incident stroke, dementia and depression, and all-cause mortality: A systematic review and meta-analysis. Neuroscience and Biobehavioral Reviews 90, 164–173. https://doi.org/10.1016/j.neubiorev.2018.04.003

Román, G.C., Erkinjuntti, T., Wallin, A., Pantoni, L., Chui, H.C., 2002. Subcortical ischaemic vascular dementia. The Lancet Neurology 1, 426–436. https://doi.org/10.1016/S1474-4422(02)00190-4

Rubinov, M., Sporns, O., 2010. Complex network measures of brain connectivity: uses and interpretations. Neuroimage 52, 1059–1069. https://doi.org/10.1016/j.neuroimage.2009.10.003

Smith, R.E., Tournier, J.-D., Calamante, F., Connelly, A., 2015. SIFT2: Enabling dense quantitative assessment of brain white matter connectivity using streamlines tractography. NeuroImage 119, 338–351. https://doi.org/10.1016/J.NEUROIMAGE.2015.06.092

Sporns, O., Zwi, J.D., 2004. The small world of the cerebral cortex. Neuroinformatics 2, 145–162. https://doi.org/10.1385/NI:2:2:145
Tournier, J.-D., Calamante, F., Gadian, D.G., Connelly, A., 2004. Direct estimation of the fiber orientation density function from diffusion-weighted MRI data using spherical deconvolution. Neuroimage 23, 1176–1185. https://doi.org/10.1016/j.neuroimage.2004.07.037
Tuladhar, A.M., Lawrence, A., Norris, David.G., Barrick, T.R., Markus, H.S., de Leeuw, F., 2017. Disruption of rich club organisation in cerebral small vessel disease. Human Brain Mapping 38, 1751–1766. https://doi.org/10.1002/hbm.23479
Tuladhar, A.M., Reid, A.T., Shumskaya, E., de Laat, K.F., van Norden, A.G.W., van Dijk, E.J., Norris, D.G., de Leeuw, F.-E., 2015a. Relationship Between White Matter Hyperintensities, Cortical Thickness, and Cognition. Stroke 46, 425–432. https://doi.org/10.1161/STROKEAHA.114.007146
Tuladhar, A.M., van Norden, A.G.W., de Laat, K.F., Zwiers, M.P., van Dijk, E.J., Norris, D.G., de Leeuw, F.-E., 2015b. White matter integrity in small vessel disease is related to cognition. NeuroImage: Clinical 7, 518–524. https://doi.org/10.1016/j.nicl.2015.02.003
van Agtmaal, M.J.M., Houben, A.J.H.M., Pouwer, F., Stehouwer, C.D.A., Schram, M.T., 2017. Association of Microvascular Dysfunction With Late-Life Depression: A Systematic Review and Meta-analysis. JAMA Psychiatry 74, 729–739. https://doi.org/10.1001/jamapsychiatry.2017.0984
Van Den Heuvel, M.P., Stam, C.J., Kahn, R.S., Hulshoff Pol, H.E., 2009. Efficiency of functional brain networks and intellectual performance. Journal of Neuroscience 29, 7619–7624. https://doi.org/10.1523/JNEUROSCI.1443-09.2009
van der Holst, H.M., Tuladhar, A.M., Zerbi, V., van Uden, I.W.M., de Laat, K.F., van Leijsen, E.M.C., Ghafoorian, M., Platel, B., Bergkamp, M.I., van Norden, A.G.W., Norris, D.G., van Dijk, E.J., Kiliaan, A.J., de Leeuw, F.-E., 2018. White matter changes and gait decline in cerebral small vessel disease. NeuroImage: Clinical 17, 731–738. https://doi.org/10.1016/j.nicl.2017.12.007
Wallin, A., Román, G.C., Esiri, M., Kettunen, P., Svensson, J., Paraskevas, G.P., Kapaki, E., 2018. Update on Vascular Cognitive Impairment Associated with Subcortical Small-Vessel Disease. Journal of Alzheimer's disease : JAD 62, 1417–1441. https://doi.org/10.3233/JAD-170803
Wardlaw, J.M., Smith, E.E., Biessels, G.J., Cordonnier, C., Fazekas, F., Frayne, R., Lindley, R.I., O'Brien, J.T., Barkhof, F., Benavente, O.R., Black, S.E., Brayne, C., Breteler, M., Chabriat, H., DeCarli, C., de Leeuw, F.-E., Doubal, F., Duering, M., Fox, N.C., Greenberg, S., Hachinski, V., Kilimann, I., Mok, V., van Oostenbrugge, R., Pantoni, L., Speck, O., Stephan, B.C.M., Teipel, S., Viswanathan, A., Werring, D., Chen, C., Smith, C., van Buchem, M., Norrving, B., Gorelick, P.B., Dichgans, M., 2013. Neuroimaging standards for research into small vessel disease and its contribution to ageing and neurodegeneration. The Lancet Neurology 12, 822–838. https://doi.org/10.1016/S1474-4422(13)70124-8
Wardlaw, J.M., Valdés Hernández, M.C., Muñoz-Maniega, S., 2015. What are White Matter Hyperintensities Made of? J Am Heart Assoc 4. https://doi.org/10.1161/JAHA.114.001140
Watts, D.J., Strogatz, S.H., 1998. Collective dynamics of 'small-world' networks. Nature 393, 440–442. https://doi.org/10.1038/30918

4 Zusammenfassung

Cerebrale Mikroangiopathie (CSVD) ist eine altersassoziierte Erkrankung, die aufgrund ihrer weitreichenden Verbreitung und klinischen Symptomatik von großer sozioökonomischer Relevanz ist. Wie CSVD zu klinischen Folgeerscheinungen führt, ist weitgehend unklar. In dieser Arbeit wurden die strukturellen Konnektome von 930 Teilnehmern der Hamburg City Health Study rekonstruiert und der Zusammenhang der Konnektivität bestimmter Faserpopulationen sowie netzwerktopologischer Parameter mit Surrogatmarkern der CSVD statistisch mittels linearer Regression analysiert. Dabei zeigte sich, dass vor allem bei subcortikalen, frontalen sowie interhemisphärischen und langen intrahemisphärischen Faserpopulationen eine verminderte Konnektivität mit erhöhter CSVD-Last einhergeht. Zudem korrespondierte eine erhöhte CSVD-Last mit einer verminderten Integration sowie erhöhten Segregation und damit einem Abweichen von der Small-world-Topologie. Die Small-world propensity korrelierte signifikant mit der Testleistung im Trail making test. Diese Resultate sprechen für eine relevante Beeinträchtigung des menschlichen Hirnnetzwerks bereits in subklinischen Stadien der CSVD und erlauben weitere Einblicke in die Pathophysiologie dieser Erkrankung.

Cerebral small vessel disease (CSVD) is an age-associated disease of great socioeconomic relevance due to its extensive prevalence and clinical symptoms. However, it is largely unclear how CSVD leads to these sequelae. In this work, the structural connectomes of 930 participants of the Hamburg City Health Study were reconstructed and the correlation of connectivity of certain fibre populations and network topological parameters with surrogate markers of CSVD were statistically analysed in a linear regression analysis. It was shown that especially in subcortical, frontal, interhemispheric and long intrahemispheric fibre populations, decreased connectivity is associated with increased CSVD load. Moreover, an increased CSVD load corresponded to reduced network integration and increased segregation and thus to a deviation from the small-world topology. The small-world propensity correlated significantly with the performance in the trail making test. These results indicate a relevant impairment of the human brain network already in subclinical stages of CSVD and provide further insights in the pathophysiology of this disease.

5 Erklärung des Eigenanteils an der Publikation

Die Daten auf denen diese Arbeit beruht wurden von den Mitarbeitern des Studienzentrums der Hamburg City Health Study erhoben. Der Eigenanteil des Doktoranden setzt an der Weiterverarbeitung der rohen Bilddaten an. In enger Zusammenarbeit mit Benedikt M. Frey, Dr. Dr. Eckhard Schlemm, Carola Mayer, PD Dr. Bastian Cheng und Prof. Dr. Götz Thomalla hat der Doktorand eine moderne sowie reproduzierbare Pipeline zur Bilddatenverarbeitung entworfen, die zum Ziel die Rekonstruktion und Konnektomen, sowie die Konzeptionalisierung und Durchführung von deren Analyse. Kurz zusammengefasst umfasste dies die Präprozessierung der Bilddaten, die Berechnung der CSVD-Surrogatmarker inklusive der manuellen Zusammenstellung eines Trainingsdatensatzes zur WMH-Segmentierung, die Rekonstruktion der Konnektome aus T1- und diffusionsgewichteten MR-Bilder mittels High-Performance Computing Cluster, die visuelle Qualitätssicherung, die Berechnung von Konnektivitätswerten und topologischen Netzwerkparametern sowie die statistische Auswertung und deren Visualisierung sowie zuletzt das Schreiben der Manuskripte.

6 Danksagung

Ein großes Dankeschön gilt den Teilnehmern und Studienzentrumsmitarbeitern der HCHS, den Mitarbeitern des Rechenzentrums der Universität Hamburg sowie dem Kreis der Koautoren für ihren großen Anteil am Projekt. Benedikt Frey, Bastian Cheng und Götz Thomalla danke ich für ihre steten Impulse, hervorragende Betreuung und Ausbildung sowie die Tatsache, dass sie meine Faszination für den Bereich der neurowissenschaftlichen Bildgebung geweckt haben. Besonderer Dank gilt meiner Familie und allen voran meiner Freundin Janina für ihre bedingungslose Liebe und Unterstützung.

7 Lebenslauf

Lebenslauf wurde aus datenschutzrechtlichen Gründen entfernt.

8 Eidesstattliche Versicherung

Ich versichere ausdrücklich, dass ich die Arbeit selbständig und ohne fremde Hilfe verfasst, andere als die von mir angegebenen Quellen und Hilfsmittel nicht benutzt und die aus den benutzten Werken wörtlich oder inhaltlich entnommenen Stellen einzeln nach Ausgabe (Auflage und Jahr des Erscheinens), Band und Seite des benutzten Werkes kenntlich gemacht habe.
Ferner versichere ich, dass ich die Dissertation bisher nicht einem Fachvertreter an einer anderen Hochschule zur Überprüfung vorgelegt oder mich anderweitig um Zulassung zur Promotion beworben habe.
Ich erkläre mich einverstanden, dass meine Dissertation vom Dekanat der Medizinischen Fakultät mit einer gängigen Software zur Erkennung von Plagiaten überprüft werden kann.

Unterschrift: .....